New Phytologist

Research

Convergently selected NPF2.12 coordinates root growth and nitrogen use efficiency in wheat and barley

Md. Nurealam Siddiqui[1,2], Kailash Pandey[1], Suzan Kumer Bhadhury[1], Bahman Sadeqi[1], Michael Schneider[3], Miguel Sanchez-Garcia[4], Benjamin Stich[2,5], Gabriel Schaaf[6], Jens Léon[1,7] and Agim Ballvora[1]

[1]Institute of Crop Science and Resource Conservation (INRES)-Plant Breeding, University of Bonn, Katzenburgweg 5, Bonn D-53115, Germany; [2]Department of Biochemistry and Molecular Biology, Bangabandhu Sheikh Mujibur Rahman Agricultural University, Gazipur 1706, Bangladesh; [3]Institute for Quantitative Genetics and Genomics of Plants, Heinrich Heine University, Düsseldorf, Germany; [4]Biodiversity and Crop Improvement Program, International Center for Agricultural Research in the Dry Areas (ICARDA), Rabat 10101, Morocco; [5]Cluster of Excellence on Plant Sciences (CEPLAS), Heinrich Heine University, Düsseldorf 40225, Germany; [6]Department of Plant Nutrition, Institute of Crop Science and Resource Conservation (INRES), University of Bonn, Karlrobert-Kreiten-Str. 13, Bonn D-53115, Germany; [7]Field Lab Campus Klein-Altendorf, University of Bonn, Klein-Altendorf 2, Rheinbach 53359, Germany

Author for correspondence:
Agim Ballvora
Email: ballvora@uni-bonn.de

Received: *31 October 2022*
Accepted: *13 February 2023*

New Phytologist (2023) **238:** 2175–2193
doi: 10.1111/nph.18820

Key words: cereals, genetic variation, genome-wide association mapping, nitrate transport, nitrogen use efficiency, root system architecture.

Summary

- Understanding the genetic and molecular function of nitrate sensing and acquisition across crop species will accelerate breeding of cultivars with improved nitrogen use efficiency (NUE).
- Here, we performed a genome-wide scan using wheat and barley accessions characterized under low and high N inputs that uncovered the *NPF2.12* gene, encoding a homolog of the Arabidopsis nitrate transceptor NRT1.6 and other low-affinity nitrate transporters that belong to the MAJOR FACILITATOR SUPERFAMILY.
- Next, it is shown that variations in the *NPF2.12* promoter correlated with altered *NPF2.12* transcript levels where decreased gene expression was measured under low nitrate availability. Multiple field trials revealed a significantly enhanced N content in leaves and grains and NUE in the presence of the elite allele $TaNPF2.12^{TT}$ grown under low N conditions. Furthermore, the nitrate reductase encoding gene *NIA1* was up-regulated in *npf2.12* mutant upon low nitrate concentrations, thereby resulting in elevated levels of nitric oxide (NO) production. This increase in NO correlated with the higher root growth, nitrate uptake, and N translocation observed in the mutant when compared to wild-type.
- The presented data indicate that the elite haplotype alleles of *NPF2.12* are convergently selected in wheat and barley that by inactivation indirectly contribute to root growth and NUE by activating NO signaling under low nitrate conditions.

Introduction

During the last decades, the breeding of cereals and other major crops has been concentrated on the selection for increasing grain yield under high-input cropping systems, which are directly responsible for ecological imbalances and cost penalties (Foley *et al.*, 2011; Garnett *et al.*, 2013; Voss-Fels *et al.*, 2019). Nitrogen (N) is often the limiting nutrient in agriculture and its application significantly increases crop yield. However, applying excess amounts of N is not productive and has negative ecological consequences (Vitousek *et al.*, 2009; Lebender *et al.*, 2014; Wang *et al.*, 2014, 2023; Chen *et al.*, 2020; Mahmud *et al.*, 2021). It has been documented that only 33–40% of the applied N can be converted into grain yield. The remaining N is lost either by nitrate (NO_3^-) leaching or depending on soil pH, redox status, and microbial activity by N_2O or NH_3 emissions all of which can result in very substantial N losses and environmental pollution (Hirel *et al.*, 2011; Dhital & Raun, 2016; Yang *et al.*, 2019). By contrast, low soil N availability is also one of the limiting factors for crop yield in many countries of the world, including sub-Saharan Africa and Latin America (Gibbon *et al.*, 2007). Therefore, there is increasing interest in developing high nitrogen use efficiency (NUE) varieties to minimize the excess costs to farmers and detrimental impacts on ecosystems (Liu *et al.*, 2003; Chen *et al.*, 2014; Tang *et al.*, 2019). Improved NUE under N-limited conditions is influenced by efficient NO_3^- transporter genes (Li *et al.*, 2016; O'Brien *et al.*, 2016; Jia *et al.*, 2019). Expanding our knowledge on convergently regulated NO_3^- transporter genes across crops and their interconnections with the processes of NO_3^- sensing, root growth, NO_3^- uptake, as well as root-to-shoot transport and assimilation will speed up the breeding of NUE in all species.

NO_3^- is the most predominant source of N in natural, as well as agricultural ecosystems (von Wirén *et al.*, 2000). Plants take

up NO_3^- by roots using NO_3^- transporters. In the next step, NO_3^- is then distributed within the plant, or is conjugated with carbon molecules to generate amino acids through assimilation before distribution (Miller *et al.*, 2007; Xu *et al.*, 2012). Besides being an essential nutrient, NO_3^- also acts as a signaling molecule that coordinates NO_3^--induced gene expression to regulate plant growth and development, especially in roots (Vidal & Gutiérrez, 2008; Krouk *et al.*, 2010; Alvarez *et al.*, 2012). In higher plants, NO_3^- uptake and transport systems consist of a low-affinity transport system (LATS) and a high-affinity transport system (HATS) that depend among others on the availability of cellular energy and proton electrochemical gradients (Siddiqi *et al.*, 1990; Miller *et al.*, 2007). Over the last two decades, five transporter families involved in NO_3^- transport were identified in plants, namely nitrate transporter 1 (NRT1), nitrate transporter 2 (NRT2), chloride channel (CLC), slow anion-associated channel homolog (SLC/SLAH), and aluminium-activated malate transporter (ALMT) (Fan *et al.*, 2017). The first plant NO_3^- transporter identified in *Arabidopsis thaliana* was NRT1.1 (also named NPF6.3 or CHL1) that belongs to the NITRATE TRANSPORTER 1 (NRT1) or PEPTIDE TRANSPORTER (PTR) family as also named as NPF proteins (Tsay *et al.*, 1993; Léran *et al.*, 2014). This family has 53 and 93 members in Arabidopsis and rice, respectively, which can be further classified into 8–10 subfamilies (Léran *et al.*, 2014; von Wittgenstein *et al.*, 2014) and display diverse substrate specificities. Although NPF members have been reported to act as the main components of the LATS at high NO_3^- concentrations (Fan *et al.*, 2017), specialized members such as NRT1.1 in Arabidopsis (Liu & Tsay, 2003) and MtNRT1.3 in *Medicago truncatula* (Morère-Le Paven *et al.*, 2011) function as dual-affinity transporters associated with both HATS and LATS. Furthermore, MtNIP/LATD in *Medicago* that belongs to NPF has been reported as a high-affinity NO_3^- transporter (Bagchi *et al.*, 2012). NPF members play important functions in N utilization (Wang *et al.*, 2018). Alterations in amino acid sequences of NPF proteins in rice have been shown to affect NO_3^- transport and NUE, suggesting that these proteins integrate a regulatory network that controls NUE and grain yield (Hu *et al.*, 2015; Tang *et al.*, 2019).

Comparative genome-wide association studies (GWAS) using multiple species have been recently used as a powerful tool to dissect genetic architecture within species and to identify candidate genes conserved in related species (Klein *et al.*, 2020; Zheng *et al.*, 2020). Among cereals, wheat and barley are both economically important crops, ranked second and fourth, respectively, in terms of their global production, and in meeting food demands in human nutrition (https://faostat.fao.org/). These two species diverged since they evolved from a common ancestor *c.* 10–14 Ma (Schreiber *et al.*, 2009). In-depth genetic mapping and structural genomic investigations revealed that both genomes are largely conserved (Devos & Gale, 1997; Schreiber *et al.*, 2009). Comparative transcriptome analyses in Triticeae indicated that highly expressed genes in wheat and barley tend to be evolutionarily conserved (Schreiber *et al.*, 2009). Therefore, convergent orthologues between related species are more likely to maintain steady functional patterns of gene regulation and expression (Davidson *et al.*, 2012). However, no studies are available so far that reported a comparative GWAS between wheat and barley to unravel shared regulators of root-to-shoot NO_3^- translocation and to analyze their allelic variations related to root growth and NUE with respect to heterogeneous N availability.

In this study, we performed genome-wide analyses using panels of winter wheat and spring barley to analyze root phenotypes under extreme N-entry levels in the field and under controlled conditions, respectively. We identified several marker-trait associations (MTAs) colocalizing with candidate genes that are involved in N transport and metabolism, and prioritized a convergently selected gene between wheat and barley that shares homology with Arabidopsis NO_3^- transceptors. We reported that natural alleles of *NPF2.12* diverge in regulatory elements and establish distinct haplotype (Hap) differences. The expression of a rare natural allele of *NPF2.12* was associated with a significantly enhanced root growth and root-to-shoot NO_3^- translocation in both crops at low NO_3^-. Furthermore, transcriptome and gene expression analyses revealed an up-regulation of *NITRATE REDUCTASE 1* (*NIA1*) in an *npf2.12* wheat mutant, which was associated with increased root growth, thereby leading to a robust NO_3^- uptake and root-to-shoot transport activity at limited NO_3^- availability.

Materials and Methods

Plant materials

The genetic material used in this study is a global collection of 221 winter wheat (*Triticum aestivum* L.) cultivars (Supporting Information Table S1). These were selected from an association panel developed in the breeding innovations in wheat for resilient cropping systems (BRIWECS) consortium in Germany as previously described (Voss-Fels *et al.*, 2019).

For barley (*Hordeum vulgare* L.), a total of 200 spring barley inbreeds that consisted of advanced breeding lines, cultivars, and landraces developed by the International Center for Agricultural Research in the Dry Areas (ICARDA) were evaluated (listed in Table S2). This diverse panel of barley genotypes was selected from the stress inputs barley breeding programs (stress in terms of limited fertilizer and moisture) of ICARDA (Amezrou *et al.*, 2018).

Field and controlled experiments

This diversity panel was evaluated in Campus Klein-Altendorf research facilities of Bonn University under natural field conditions in three consecutive growing seasons from 2017 to 2018, from 2018 to 2019, and from 2019 to 2020, under high dose N, HN (220 kg N ha^{-1}, fertilizer adjusted based on soil mineral nitrogen, N_{min}) and no artificial nitrogen-supply as low dose N (LN), (0 kg N ha^{-1}) conditions, where the experiments were performed in different fields. The experimental design and management practices were followed as previously described (Voss-Fels *et al.*, 2019), except fungicide application. Fertilizer and lime

applications were made following the soil test results to adjust the nutritional levels previously described (Table S3). At flowering stage (BBCH65), root systems of at least three representative plants from each plot were harvested using the '*Shovelomics*' approach (Trachsel *et al.*, 2011; Oyiga *et al.*, 2020).

Sixteen seeds of each barley inbreed were placed in transparent plastic boxes (29 × 22.5 cm) containing blotting paper (Albet Lab Science, Dassel, Germany) soaked in 50 ml of a solution containing two levels of NO_3^- as N Ion Chromatography Standard (H_2O, $NO_3^{(-)}$ as N: 1000 μg ml^{-1}), supplied with either 10 mM (HN) or 0.5 mM NO_3^- (LN). The plastic box was kept in dark conditions at 4°C for 48 h to stimulate the germination process and then placed in a growth chamber (Bronson Climate, LW Zaltbommel, the Netherlands) with white fluorescent light (600 μmol m^{-2} s^{-1}; 14 h : 10 h, light : dark) at 23°C ± 1°C, and relative humidity of 65 ± 8%. The experiment was repeated at least two times so that a total of eight uniform plants were obtained per genotype per NO_3^- level. The 14-d-old seedlings of identical size for each barley genotype were harvested, and roots were carefully separated from shoot. The rooting depth was determined using a meter scale from root–shoot junction to root apex. After that, root samples were preserved in plastic pot containing 60% alcohol (v/v) for further root phenotyping.

Root phenotyping

The preserved root samples were properly placed in the scanner tray and adjusted vertically on scanning plates to avoid overlapping roots. Next to a ruler, an eight-bit gray scale image was generated using a high-resolution Epson scanner (Perfection LA24000) maintaining a resolution of 600 dots per inch (Kadam *et al.*, 2017). Root morphological traits were quantified by analyzing the root images with WinRhizo analysis system (v.2020a; Regent Instruments Inc., Quebec, Canada; Fig. S1).

To investigate the root anatomical structures, well-cleaned and preserved root samples from main shoot and tiller nodal roots were free-hand sectioned using a razor blade (Apollo, Solingen, Germany) at 1 cm position from root–shoot junction (Oyiga *et al.*, 2020). Two root images from three individual plants per replicate were acquired by the digital microscope (VHX-1000D; Keyence's, Germany) with ×50 and ×100 magnification. The ratio of image pixels to the scale bar length was adjusted during image analysis by the ImageJ (v.1.52a) software. The diameter of the whole cross-section, the cortical cell, the stele, and the metaxylem vessels was measured to convert the pixel counts to diameter (μm; Schneider *et al.*, 2012; Kadam *et al.*, 2017). The water conductance parameter in terms of axial hydraulic conductivity was measured as described (Kadam *et al.*, 2015). The list of all traits with description is provided in Table S4.

SNP genotyping

For wheat, 24 216 single-nucleotide polymorphisms (SNP) markers were obtained by extracting DNA from the 221 wheat cultivars and those genome-wide SNP markers as described by Voss-Fels *et al.* (2019) and Dadshani *et al.* (2021). For barley, a total of 23 805 SNPs were obtained using 50K iSelect SNP array based on Illumina's Inifinium Assay (Illumina, San Diego, CA, USA; Bayer *et al.*, 2017). Wheat and barley SNPs data were curated before data imputation using Tassel v.5.2.61, where SNP loci and individuals with < 10% missing values and rare SNPs with < 5% minor allele frequencies (MAF) were excluded from the data following Bayer *et al.* (2017) and Voss-Fels *et al.* (2019), respectively.

Comparative GWAS between wheat and barley

The SNPs involved with the alteration in root system traits induced by N levels were identified by adopting GWAS using mixed linear model (MLM; Stich *et al.*, 2008). Here, root traits were considered as phenotypes, whereas the confounding effects of population stratification in both panels were employed by incorporating population structure (P-matrix principal component analysis) and kinship (K-matrix) as covariates (Kang *et al.*, 2010). The P- and K-Matrix were assembled using Tassel (v.5.2.61). Genome-wide association study was also conducted in Tassel, using the model: $y = X\beta + Zu + e$, where y considered as the vector of phenotypic traits; X is the corresponding SNP vector; β is the coefficient factors for SNP effect, Z represents the corresponding design matrix; u indicates random effects computing for populations structure and kinship; and e is a vector of random error (Kang *et al.*, 2010). The false discovery rate (FDR) adjusted P-value (q-value) of 0.01 was calculated using the qvalue package (Storey *et al.*, 2020). Significant MTAs were considered when FDR q-values below the FDR ≤ 0.01 threshold were noticed. Manhattan and Quantile–Quantile (Q–Q) plots were generated in R using the qqman package, based on Tassel summary statistics.

To obtain wheat candidate genes, we additionally performed linkage disequilibrium (LD) analysis based on significant SNPs identified by GWAS using Haploview (v.2.4) as described previously (Siddiqui *et al.*, 2021a). Parameter r^2 value was considered to determine the degree of LD (Li *et al.*, 2016). All the associated significant SNPs in high chromosomal LD region with each other were defined to be linked (SNP-clusters). The LD blocks containing significant SNPs were considered as candidate loci. The significant SNPs that did belongs to LD blocks were treated differently. All candidate genes within ±1 Mbp of the corresponding SNPs were annotated using the International Wheat Genome Sequencing Consortium (IWGSC) RefSeq v.1.0 in the URGI wheat database (https://wheat-urgi.versailles.inra.fr; Alaux *et al.*, 2018). For barley, core sequences of the significant markers were Blast searched using the public Barley Genome Gene-set database (EnsemblPlants; https://plants.ensembl.org). Top gene hits were determined by considering scores of > 80% similarity and e-values < 1e-70 (Oyiga *et al.*, 2020). The annotated high confidence (HC) genes (genes with known annotation and verified positions on the WGS assembly of cv Morex (Larkin *et al.*, 2007; IBGC, 2012) were searched in the IPK Barley Genome database (https://apex.ipk-gatersleben.de/apex/f?p=284:41:::NO:RP:P41_GENE_CHOICE:2). Wheat and barley syntenic genes were curated following the methods by Zhang *et al.* (2017)

adopting the reference genomes IWGSC RefSeq v.1.0 for wheat and IBSC_v2 for barley in EnsemblPlants database (https://plants.ensembl.org).

Phylogenetic analysis

The NPF2.12 protein domains were analyzed using BLASTP (protein–protein BLAST). The full-length protein sequences of *NPF2.12* orthologs in the Arabidopsis genus were sequenced from BLAST search online database (Table S5). The multiple-sequence alignment and phylogenetic tree were constructed by CLUSTALW2 (https://www.ebi.ac.uk/Tools/msa/clustalw2/; Larkin *et al.*, 2007).

Candidate gene sequence analysis

Whole genomic DNA of selected genotypes (Tables S6, S7) was extracted from leaves using a peqGOLD Plant DNA Mini Kit (VWR Life Science, USA). An *c.* 1.5-kb region upstream from the start codon ATG of *TaNPF2.12* and *HvNPF2.12* was considered as promoter region (Muzammil *et al.*, 2018). Primers (Tables S8, S9) were designed and synthesized by Sigma-Aldrich (Merck KGaA, Darmstadt, Germany). The region of interest was amplified by polymerase chain reaction (PCR) using One *Taq* 2X Master Mix (New England, BioLabs). The cycling conditions were followed by Muzammil *et al.* (2018). The amplified PCR products were purified by a FastGene Gel/PCR Extraction Kit (Nippon Genetics, Tokyo, Japan). DNA sequences were aligned and compared using DNASTAR 'SeqMan Pro' v.12.0.0 (www.dnastar.com) to detect possible polymorphic sites.

Isolation of RNA and RT-qPCR analysis

Total RNA isolation from the harvested all root parts of wheat and barley plants (root samples immediately frozen with liquid N) were performed after 14 d in high NO_3^-–N (10 mM) and low NO_3^-–N (0.5 mM) conditions using Monarch Total RNA Miniprep Kit (BioLab) according to the manufacturer's guidelines. The RT-qPCR reaction mixture (20 µl) consisted of 10 µl master mix and 1 µl enzyme mix (supplied in the kit), 0.8 µl each of forward and reverse gene-specific primers (primers list in Tables S8, S9), 5.4 µl nuclease-free water, and 2 µl template RNA. The Luna Universal One-Step RT-qPCR Kit (NEB #E3005L) was used for the analysis. The gene expression levels were calculated using $\Delta\Delta C_t$ values and expressed as fold change relative to the stably expressed two internal control genes, *TaEf-1a* and *TaEf-1b* (Unigene accession no. Ta659) for wheat and *Ef1-a* for barley.

Evaluation of NUE-related traits of *TaNPF2.12* alleles under field conditions

The 10 wheat cultivars containing $TaNPF2.12^{CC}$ and $TaNPF2.12^{TT}$ from each allele group (Table S6) were grown in field conditions across three cropping systems in 2017–2018, 2018–2019, and 2019–2020. The seeds of each genotype were sown in a plot (7 × 3 m) distributed as split plot design with two replications (organized in randomized block design). The selected cultivars were grown under two different N levels (HN and LN) as mentioned above for wheat cultivation previously described by Voss-Fels *et al.* (2019), except fungicide application. After harvest, total N contents in dry grinded leaves and grains were determined using the near-infrared spectrometer (NIRS) with Diode Array 7250 NIR analyzer (Perten Instruments Inc., USA) as described by Koua *et al.* (2021). N uptake efficiency (NUpE) was determined by the ratio of the total aboveground N at the by the total N available in soil and NUE was estimated by the ratio of total grain yield to applied N fertilizer as defined by Moll *et al.* (1982).

^{15}N-label NO_3^- uptake and translocation assay

Two-week-old of *TaNPF2.12* and *HvNPF2.12* (Hap1 and Hap2) in wheat and barley, wild-type (WT) and *npf2.12* of wheat seedlings grown in Hoagland nutrient solution were used for $^{15}NO_3^-$ uptake and translocation assays as followed by Liu *et al.* (2016). All plants were exposed to N starvation solution for 3 d before $^{15}NO_3^-$ treatment. After 2 wk, roots were washed by tap water twice and then seedlings were again exposed to Hoagland nutrient solution containing 0.5 or 5 mM ^{15}N-labelled KNO_3 (generated from a stock solution containing 99.3% $K^{14}NO_3$ and 0.7% $K^{15}NO_3$; Sigma) for 3 h. After rinsed with 0.1 mM $CaSO_4$ for 1 min, roots and shoots were harvested separately, and oven-dried at 70°C for 72 h, followed by dry weight (DW) measurements. ^{15}N contents in roots and shoots were analyzed by GC–MS (ANCA-SL/2020; Europa Scientific/Sercon Ltd, UK). The activities of ^{15}N–NO_3^- uptake and root-to-shoot transport activity were calculated based on the equation described by Liu *et al.* (2016).

Transcriptome analysis

The *npf2.12* mutant of durum wheat (*Triticum turgidum*) were purchased from a TILLING population generated in tetraploid cv Kronos background (Krasileva *et al.*, 2017). The TILLING line (Kronos4652) possessed premature termination codons in the *npf2.12* homologous coding sequences of *TraesCS3B02G454000*. The mutated seeds were selfed to F_5 to fix the mutations. The *npf2.12* mutant and WT seedlings were grown in transparent plastic boxes (29 × 22.5 cm) with blotting paper and irrigated with the solution containing 10 (high) and 0.5 (low) mM NO_3^-–N weekly. The roots of the *npf2.12* mutant and WT plants were collected after 14 d of NO_3^-–N impositions. Total RNA was extracted using the Monarch Total RNA Miniprep Kit (BioLab). The library preparation and sequencing were conducted by NGS Core Facility at the University of Bonn, Germany (https://btc.uni-bonn.de/ngs). RNA sequencing reaction performed using the QuantSeq 3′-mRNA-Seq Kit from Lexogen and sequenced on an Illumina NovaSeq 6000 platform. Three biological replicates for each treatment were used and for each replicate 14 million reads were sequenced. The transcriptome data analysis was illustrated in Methods S1.

Quantification of NO, NR activity and NO_3^-–N and total N contents

The WT and mutant lines were grown in transparent plastic boxes containing blotting paper in a growth chamber applied either high (10 mM) or low (0.5 mM) NO_3^-–N as mentioned above. The nitric oxide (NO) contents and nitrate reductase (NR) activity were determined in the fresh root samples harvested after 14 d of NO_3^-–N treatments using NO Assay Kit from Abnova (KA1641) and NR Assay Kit from Biorbyt (0rb219870), respectively, following the manufacturer's protocols.

Determination of NO_3^-–N contents was performed as described by Cataldo *et al.* (1975). Freshly harvested roots and shoots were homogenized using 5 ml of boiling water to 0.1 g tissue samples and then tubes were boiled in a water bath for 10 min (Ligero *et al.*, 1987). An aliquot of 0.2 ml extract was mixed with 0.8 ml of 5% salicylic acid in concentrated H_2SO_4 and then incubated for 20 min. In the following step, 19 ml of 2 M NaOH was added and then absorbance was taken in a spectrophotometer at 410 nm. Total NO_3^-–N concentrations in root and shoot were represented as μmol NO_3^-–N per g fresh weight. For total N contents estimation, separated roots and shoots were oven-dried at 65°C for 72 h, and then finely grinded samples were again oven-dried at 65°C for overnight. Total N contents were quantified by an elemental analyzer (Euro-EA 3000; Euro-Vector SpA, Italy).

Statistical analysis

For descriptive statistics, two-way analysis of variance (ANOVA) was performed using MLM, where genotypic and treatment effects were considered as fixed effects with their interaction, and block and replications were treated as random effects (Siddiqui *et al.*, 2021a). The broad-sense heritability (H^2) was calculated following the equation by Johnson *et al.* (1955). Binary comparisons of data were statistically analyzed following Student's *t*-test ($P < 0.05$; $P < 0.01$). For multiple comparisons between WT, mutant and haplotype lines, one-way ANOVA followed by post hoc Tukey's test at $P < 0.05$ and $P < 0.01$. All statistical analyses were conducted in R (R Core Team, 2013).

Results

N-induced divergence of root phenotypes in wheat and barley populations

A winter wheat panel comprising 221 cultivars registered in Europe from 1963 to 2013 was used in this study. The majority of cultivars were of German origin (60%), while the remaining originated from 25 different countries. This diversity panel has previously been used for several GWAS (Voss-Fels *et al.*, 2019; Begum *et al.*, 2020; Koua *et al.*, 2021; Siddiqui *et al.*, 2021a). For this study, we acquired phenotypic data for 21 root system-related traits (Table S4) under two contrasting environments in the field: low N (LN) conditions in which no mineral N was added, and high N (HN) where 220 kg N ha^{-1} were added. Under LN conditions, significantly increased trait values for root morphological traits such as total root length (TRL), root surface area (RSA), root volume (RV), and number of root tips (RT; Tables S10, S11) were observed. By contrast, HN conditions led to a significant decrease in most of the anatomical traits, except in some ratio-based anatomical traits, such as percentage of main shoot nodal root cross-section occupied by stele (mSDP) and percentage of tiller nodal root cross-section occupied by stele (tSDP), respectively. All of the traits showed significant genotype-treatment interactions (Table S10). Under HN supply, all 21 root-related traits exhibited a decreasing phenotypic variability, and their coefficients of variations were > 20 and 10% for morphological and anatomical traits, respectively (Table S10). The broad-sense heritability (H^2) of root traits under HN supply showed low ranges between 56 and 81% when compared to LN supplied grown plants (Table S11).

The barley diversity panel was phenotyped in transparent plastic boxes placed in a growth chamber and supplied with HN (10 mM NO_3^-) and LN (0.5 mM NO_3^-). Root phenotyping was carried out 14 d after imposing the treatment. The data showed that at LN supply, root morphological attributes, importantly rooting depth (RD), TRL, number of tips, forks and crossings were significantly increased than HN supply. For RSA, root average diameter (RAD), and RV, decreasing trends were detected upon LN supply when compared with HN supply (Table S12). The coefficient of variations among all of the measured root traits were > 15%, and ranged between 15 and 64%. Heritability (H^2) ranged from 23 to 68% among morphological traits under LN, which was higher than in the HN condition (Table S12). This trend indicated that both wheat and barley association panels may harbor substantial natural variations of root traits that confer efficient N-uptake and transport under LN availability.

Candidate genes involved in root growth variations and N responses

To identify genetic factors involved in the variation of the above-described root phenotypic traits in wheat and barley, we carried out a GWAS using a MLM that corrects for the confounding effects of population structure and family relatedness. We used the significance threshold of $-\log_{10}(P) > 4.0$, as defined by a previous study using the same association panel (Siddiqui *et al.*, 2021a). A total of 70 MTAs were identified for root architectural and anatomical traits under different levels of N, such as HN, LN, and LN/HN conditions across the wheat genome (Table S3). To unravel the candidate genes underlying these MTAs, we identified 37 LD blocks with 340 plausible candidate genes (Table S14). A total of 38 of them were annotated as genes involved in the metabolism, sensing, assimilation, and transport of N (Table S15). Notably, we detected a hot spot on chromosome 3B that carries several candidate genes related to N and NO_3^- responses (Table S15).

Using the same significance threshold ($-\log_{10}(P) > 4.0$), a total of 43 MTAs were identified across all the barley chromosomes, except 4H and 7H, under various NO_3^- treatments such

as HN, LN, and LN/HN (Table S16). The analyses of the genomic regions of the 43 MTAs revealed that most of them include genes related to transporter families and transcription factors (Table S16). Of them, one gene encoded a member of the NRT protein family (Table S16).

Comparative genome-wide scan between wheat and barley uncovers a convergently selected gene associated with NO_3^- sensing and acquisition

Due to the conserved relationship between wheat and barley genomes (Salse *et al.*, 2009; Schreiber *et al.*, 2009; Siddiqui *et al.*, 2021b), as well as shared patterns of root system development (Brenchley & Jackson, 1921), we hypothesized that both species may have a convergent regulation of root growth and NO_3^- sensing. To test this hypothesis, we conducted a comparative analysis between the chromosomal intervals harboring the MTAs for root system traits of wheat and barley. Based on the FDR threshold ≤ 0.01, three pairs of orthologous genes were identified on chromosome 3 within 20-kb windows surrounding the respective SNPs between wheat and barley (Table S17). A permutation analysis revealed that the occurrence of these genes was unlikely to have occurred by chance ($P = 1e\text{-}04$). In this study, we focused on *TraesCS3B02G454000* that was annotated in wheat as low-affinity NO_3^- transporter (GO: 0080054, GO: 0015706) and located adjacent to the SNP that was significantly associated with RV under LN/HN conditions. Its orthologous gene in barley, *HORVU3Hr1G092870*, encodes for a low-affinity NO_3^- transmembrane transporter homolog (NRT1/PTR FAMILY 2.13) and was detected in our GWAS by a SNP for TRL at LN/HN conditions (Fig. 1a). We defined this convergently selected gene pair as *TaNPF2.12* in wheat and *HvNPF2.12* in barley based on their closest homolog in *A. thaliana AtNRT1.6* (At1G27080). The alleles with minor frequency ($n = 49$ in wheat and 33 in barley) of both shared markers across wheat and barley showed significantly higher RV and TRL than the major alleles (Fig. 1b,c). Interestingly, all of the identified convergently selected genes between wheat and barley were associated with root morphological traits under LN/HN conditions (Table S17).

Next, we performed phylogenetic analyses with 32 NPF/NRT proteins from different plant species, including cereals. This revealed that the barley HvNPF2.12 (KAE8800431.1) was highly similar to the wheat TaNPF2.12 protein (KAF7025301.1) (Fig. S2a) and that both NPF proteins in wheat and barley share a conserved domain structure, namely that of the Major Facilitator Superfamily (MFS) (Figs 1d, S2b).

Natural allelic variations at the *NPF2.12* promoter modulates root growth, NO_3^- uptake and translocation capacity in dependence of its availability

To validate the involvement of *TaNPF2.12* in root growth and NO_3^- acquisition in wheat, a 1.5-kb region upstream of the translational start and full-length coding regions of *TaNPF2.12* of 20 NO_3^--tolerant (higher RV under LN/HN) and 20 NO_3^--sensitive (lower RV under LN/HN) wheat cultivars were sequenced and compared (Table S6). Two distinct Hap groups were observed in the *TaNPF2.12* promoter sequence among these 40 cultivars, namely Hap1 and Hap2, present in 18 and 22 cultivars, respectively (Fig. 2a). The allelic variations between Hap1 and Hap2 were detected at −1299, −1282, −1275, −1267, −1266, −1264, and −88 bp of *TaNPF2.12* (Fig. 2a), whereas no variations were observed in the coding regions. The majority of the selected NO_3^--sensitive cultivars harbor the Hap1 allele. We observed highly significant differences ($P = 3.16e\text{-}11$, Student's *t*-test) in RV between inbreeds carrying Hap1 and Hap2, with an average RV of < 1.0 and > 3.0, respectively (Fig. 2b). Furthermore, two cultivars with Hap1 carrying the CC allele of *NPF2.12* and two cultivars with Hap2 harboring the TT allele (Table S6) were selected to examine the levels of gene expression. The expression levels of *TaNPF2.12* in roots were significantly higher for the Hap1 allele (CC) of *TaNPF2.12* than for the Hap2 allele (TT) under LN (0.5 mM NO_3^-) conditions, whereas similar expression levels were observed under HN (10 mM NO_3^-) between the two Hap groups (Fig. 2c). In shoots, only the accession Basalt carrying the Hap1 allele displayed significantly higher *TaNPF2.12* expression under LN, while in the other cultivars, no significant differences in gene expression were detected between the Hap groups (Fig. S3a). By contrast, Hap2-harboring genotypes showed significantly higher TRL, RSA, RV, RT, and NO_3^- contents in roots and shoots than Hap1 genotypes at LN, while varying responses were observed at HN concentrations (Figs 2d–h, S4a,b). To investigate whether the Hap2 allele also modulates NO_3^- transport, we carried out a short-term ^{15}N-label experiment and estimated NO_3^- uptake and translocation capacity using either 5 or 0.5 mM ^{15}N-labeled KNO_3 for 3 h (0.7% of the NO_3^- was present as $^{15}NO_3^-$). ^{15}N feeding analysis showed that the plants carrying the Hap2 allele significantly increased ^{15}N content in shoots and root-to-shoot transport activity as compared to Hap1 genotypes, especially under low KNO_3 availability (Fig. 2i–l).

To estimate the allelic variations of *HvNPF2.12* in barley, the full-length coding and 1.5-kb promoter regions in 40 barley genotypes were also sequenced and compared (Table S7). Alike wheat, two Hap groups were observed with variations specifically in the 1.5 kb region upstream of the start codon (Fig. 3a). Fifteen NO_3^--sensitive genotypes (lower TRL under LN/HN) carried Hap1 and 25 NO_3^--tolerant genotypes (higher TRL under LN/HN) the Hap2 allele (Fig. 3a). The average TRL of genotypes carrying Hap2 was > 1.75, while the average TRL of inbreeds carrying Hap1 was significantly lower with 0.75 at LN/HN conditions (Fig. 3b). In the next step, we tested *HvNPF2.12* expression levels in two barley genotypes carrying the Hap1 allele and two genotypes with the Hap2 allele (Table S7). At LN availability, higher levels of *HvNPF2.12* expression were detected in roots of Hap1 (CC) genotypes than in Hap2 (TT) genotypes (Fig. 3c). In shoots, nonsignificant differential expression was observed between the Hap groups, except for Massine containing Hap2 that showed significantly lower expression under LN than under HN conditions (Fig. S3b). Notably, plants carrying the Hap2 allele (AA) showed significantly higher root growth-related traits, except RV for Massine and NO_3^- contents in shoots at LN when

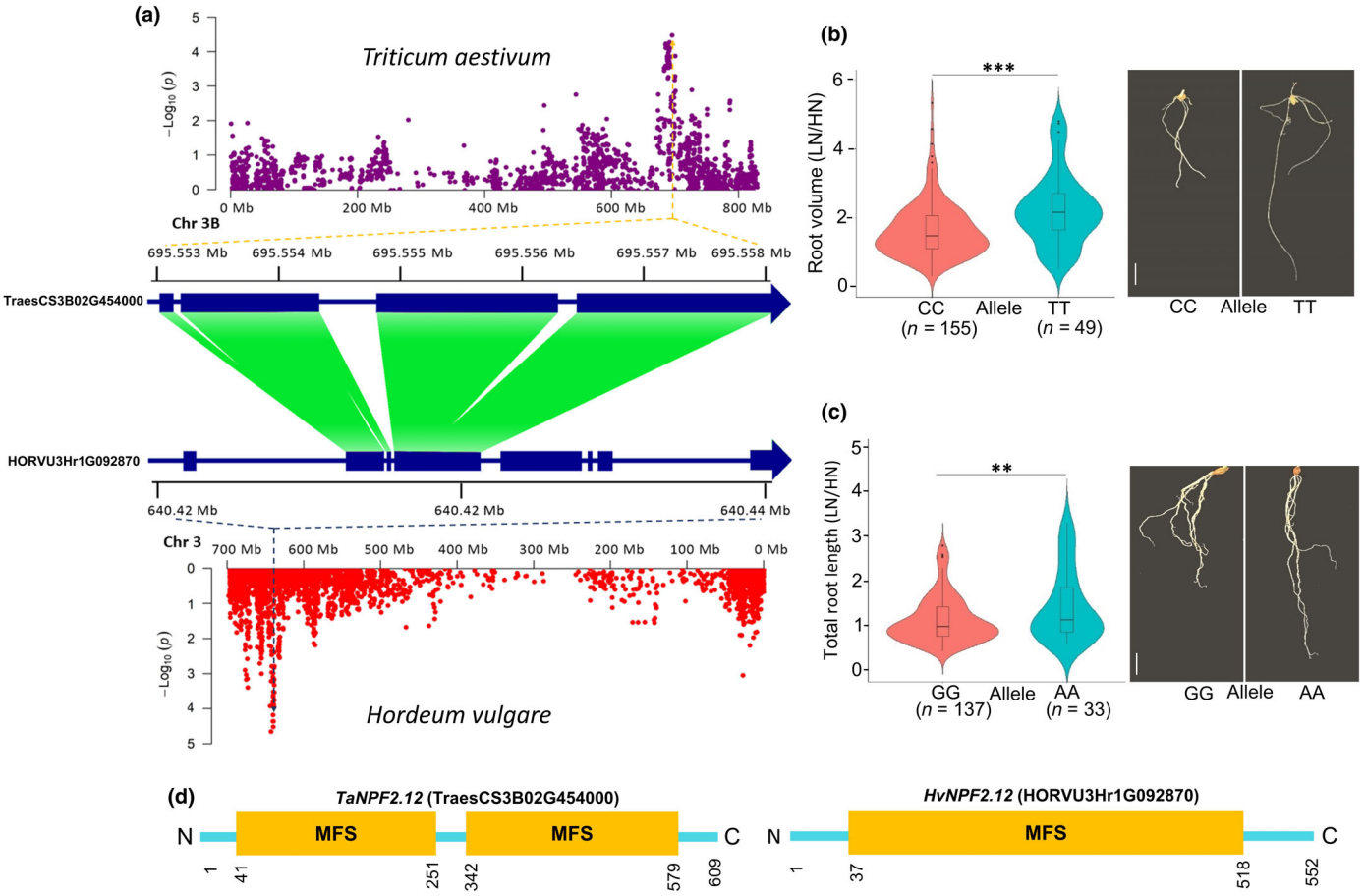

Fig. 1 Comparative genome-wide association studies (GWAS) between wheat and barley for root volume (RV) and total root length (TRL) at low dose N (LN)/high dose N (HN). (a) Manhattan plots of chromosome 3 from single-nucleotide polymorphisms (SNP)-based GWAS for RV of wheat (upper) and TRL of barley (lower) revealed a pair of convergently selected NO_3^- transporter genes; homologous sequences are highlighted in green; (b) allelic distribution and effect of wheat (left) and wheat root phenotypes (right); Anthus (cc) and Oakley (TT) alleles of the SNPs associated with RV; (c) allelic distribution and effect of barley (left) and barley root phenotypes (right); Gada (GG) and Harmal-02 (AA) alleles of the SNPs associated with TRL; (d) schematic depiction of wheat TaNPF2.12 (TraesCS3B02G454000) protein and barley HvNPF2.12 (HORVU3Hr1G092870) protein sequences representing relevant protein domains of major facilitator superfamily. Numbers denote the amino acid position in the respective proteins. In boxplots, the horizontal line at the center of the box represents the median, the center box represents the interquartile range and the thin black vertical line represents the rest of the distribution, except the circles that are determined to be potential outliers. Student's *t*-test: **, $P < 0.01$; ***, $P < 0.001$. Bars, 1 cm. NO, nitric oxide.

compared with Hap1 genotypes (Figs 3d–h; S4c,d). Interestingly, the genotype Massine harboring the Hap2 allele displayed a significantly higher ^{15}N accumulation in shoots, NO_3^- uptake, and root-to-shoot transport activity than the cultivar Gada carrying Hap1 when grown in a low KNO_3 concentration (Fig. 3i–l). Our findings in wheat and barley indicate that the Hap2 allele had lower expression levels of *TaNPF2.12* and *HvNPF2.12* than Hap1, which might lead to increased root growth and NO_3^- translocation into the shoot in response to LN availability.

Haplotype 2 allele of *TaNPF2.12*^{TT} enhances NUpE and NUE under field conditions

Field experiments were performed to analyze the allelic effects of *TaNPF2.12* on NUE-related traits. The cultivars harboring CC (Hap1) and TT (Hap2) alleles were grown in the field supplied with HN (220 kg N ha^{-1}) and LN (0 kg N ha^{-1}) levels over three consecutive cropping seasons. The N content in leaves of plants carrying the TT allele increased by 7.30% in 2017–2018 and by 6.17% in 2019–2020 as compared to the CC allele under LN input levels, while no significant differences in N content were observed under LN in 2018–2019 (Fig. 4a–c). No significant changes in N content were observed between the *TaNPF2.12* alleles under HN input levels (Fig. 4a–c). Correspondingly, the N content in grains of the genotypes carrying the TT allele was consistently increased under LN input levels over 3 yr compared with the cultivars carrying the CC allele (Fig. 4d–f). The wheat cultivars harboring the TT allele of *TaNPF2.12* exhibited significantly higher NUpE than the allele of CC under LN supply in 2018–2019 and 2019–2020, while no significant changes in NUpE were observed under HN over the three growing seasons (Fig. 4g–i). Importantly, the cultivars possessing the TT allele of *TaNPF2.12* significantly increased NUE in all three trials as compared to the CC cultivars at LN conditions (Fig. 4j–k). These results illustrate that the presence of the wheat allele

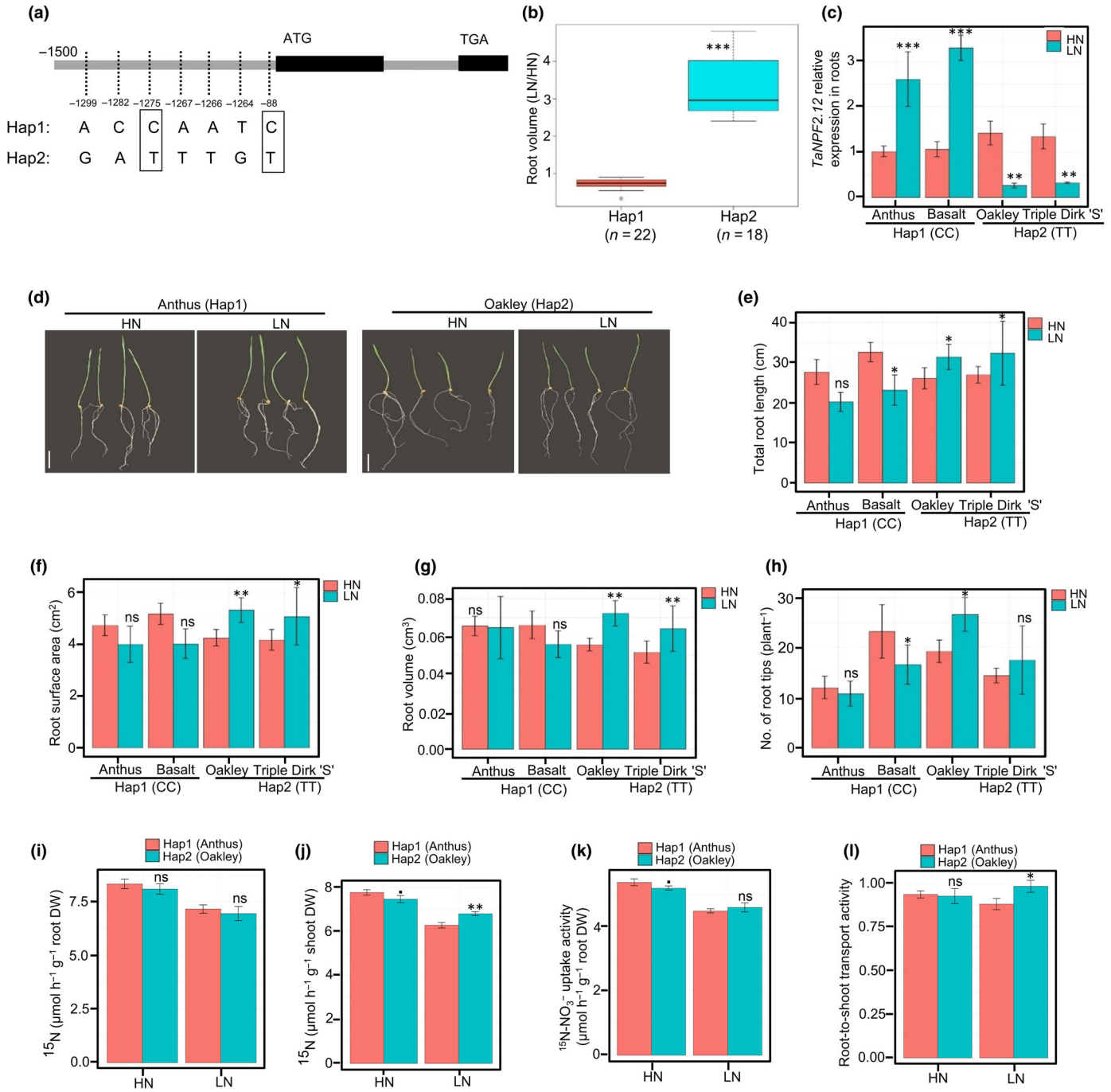

Fig. 2 Haplotype, relative expression, and root growth analyses of *TaNPF2.12* in wheat. (a) Schematic graph reveals the single-nucleotide polymorphisms (SNP) sites in the promoter regions of the *TaNPF2.12* gene and the corresponding two haplotypes, Hap1 and Hap2 (the square boxes indicate identified SNP in genome-wide association studies (GWAS)); (b) boxplot of root volume ratio for two identified haplotype groups. Statistical significance (***, $P < 0.001$) of the difference between two haplotypes was obtained by Student's *t*-test. In boxplots, the horizontal line inside of the box represents the median, the whole box represents the interquartile range and the upper and lower whiskers represent scores outside the middle 50%; (c) relative expression of *TaNPF2.12* in roots of two wheat cultivars from Hap1 (cc) and two from Hap2 (TT) alleles in response to high dose N (HN) (10 mM) and lose dose N (LN) (0.5 mM NO_3^-). The relative expression of *TaNPF2.12* in wheat roots at 14-d at LN was quantified by qRT-PCR, using *TaEf-1a* and *TaEf-1b* as the internal control genes and the corresponding samples under HN supply as controls. Data illustrate the mean ± SE of three replicates; (d–h) phenotypic differences of root systems; (e) total root length; (f) root surface area; (g) root volume; (h) number of root tips of Hap1 (CC) and Hap2 (TT) allele plants grown in a growth chamber (Bronson CLIMATE) with white fluorescent light (600 μmol m^{-2} s^{-1}; 14 h : 10 h, light : dark) at 23°C ± 1°C, and relative humidity of 65 ± 8% under HN and LN supply. Bars represent mean ± SE (n = 06 independent biological replicates); (i) ^{15}N–NO_3^- accumulation in roots; (j) ^{15}N–NO_3^- accumulation in shoots (k) ^{15}N-NO_3^- uptake and (l) root-to-shoot transport activities of Hap1 (CC) and Hap2 (TT) alleles when exposed to either 5 mM (HN) or 0.5 mM (LN KNO_3) ^{15}N-labeled KNO_3 for 3 h. Bars represent mean ± SE (n = 03 independent biological replicates). Student's *t*-test: •, $P < 0.1$; *, $P < 0.05$; **, $P < 0.01$; ***, $P < 0.001$ based on one-way ANOVA. Bars, 1 cm. NO, nitric oxide; ns, not significant.

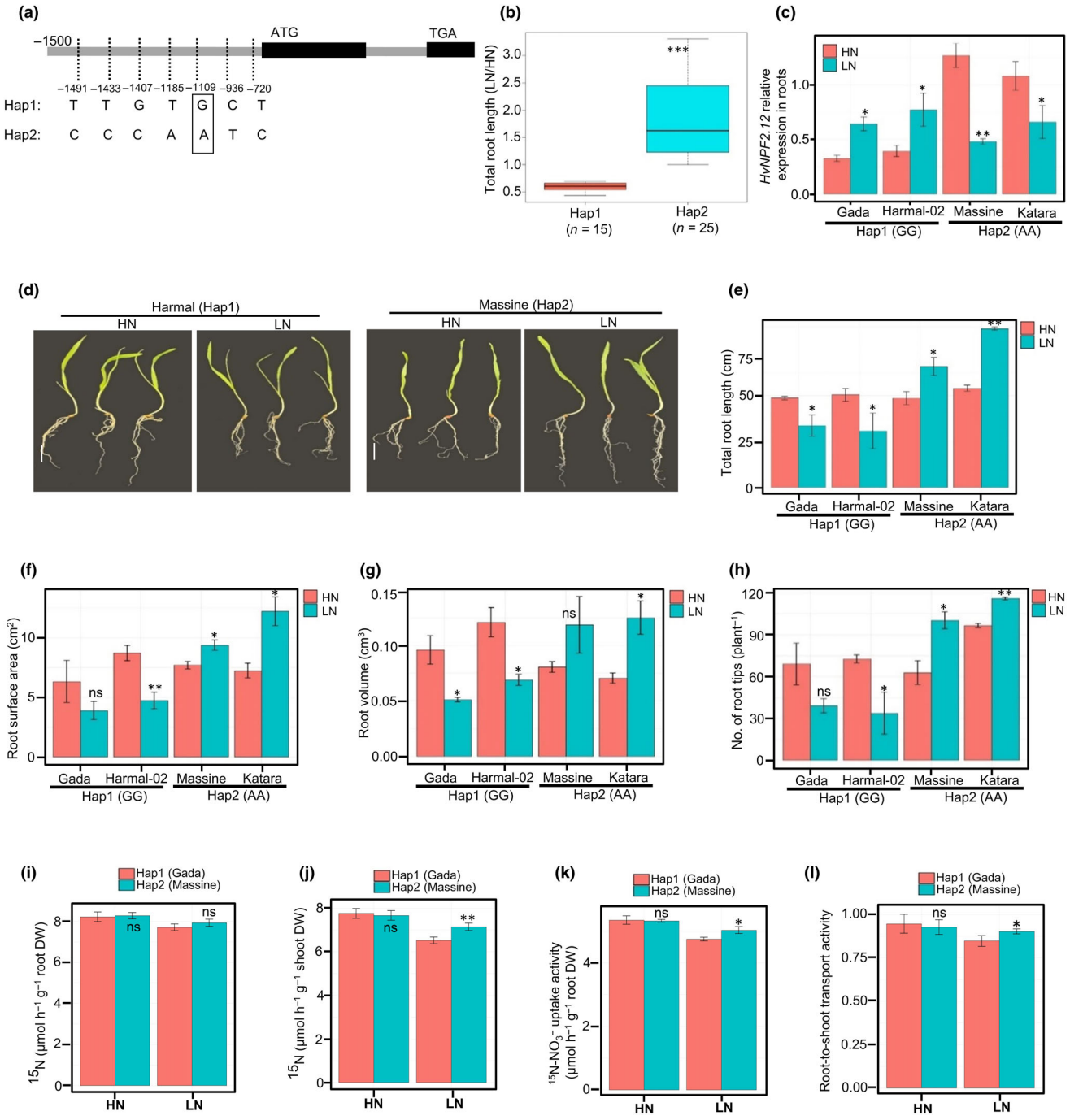

Fig. 3 Haplotype, relative expression, and root growth analyses of *HvNPF2.12* in barley. (a) Schematic graph reveals the single-nucleotide polymorphisms (SNP) sites in the promoter regions of the *HvNPF2.12* gene and the corresponding two haplotypes, Hap1 and Hap2 (the square box indicates identified SNP in genome-wide association studies (GWAS)); (b) boxplot of total root length ratio for two identified haplotype groups. Statistical significance (***, $P < 0.001$) of the difference between two haplotypes was obtained by Student's *t*-test. In boxplots, the horizontal line inside of the box represents the median, the whole box represents the interquartile range and the upper and lower whiskers represent scores outside the middle 50%; (c) relative expression of *HvNPF2.12* in roots of two barley genotypes from Hap1 (GG) and two from Hap2 (AA) alleles under high dose N (HN) (10 mM) and low dose N (LN) (0.5 mM NO_3^-) levels. The relative expression of *HvNPF2.12* in barley roots at 14 d after NO_3^- imposition at LN and was quantified by qRT-PCR, using *Ef-1a* as the internal control gene and the corresponding samples under HN supply as controls. Data illustrate the mean ± SE of three replicates; (d–h) phenotypic differences of root systems; (e) total root length; (f) root surface area; (g) root volume; (h) number of root tips of Hap1 (GG) and Hap2 (AA) allele's plants grown in a growth chamber (bronson CLIMATE) with white fluorescent light (600 μmol m^{-2} s^{-1}; 14-h : 10-h, light : dark) at 23 ± 1°C, and relative humidity of 65 ± 8% at HN and LN availability. Bars represent mean ± SE ($n = 05$ independent biological replicates). (i) ^{15}N–NO_3^- accumulation in roots; (j) ^{15}N–NO_3^- accumulation in shoots (k) ^{15}N–NO_3^- uptake and (l) root-to-shoot transport activities of Hap1 (GG) and Hap2 (AA) alleles when exposed to either 5 mM (HN) or 0.5 mM (LN KNO_3) ^{15}N-labeled KNO_3 for 3 h. Bars represent mean ± SE ($n = 03$ independent biological replicates). Student's *t*-test: •, $P < 0.1$; *, $P < 0.05$; **, $P < 0.01$; ***, $P < 0.001$ based on one-way ANOVA. Bars, 1 cm. NO, nitric oxide; ns, not significant.

TaNPF2.12^{TT} confers enhanced levels of N content in leaves and grains, which ultimately resulted in increased NUE under LN availability over three successive field trials.

A mutant allele of *TaNPF2.12* is associated with increased root growth, NO_3^- uptake, and root-to-shoot transport

To investigate consequences of *TaNPF2.12* deficiency on root growth and NO_3^- transport, we employed an *npf2.12* wheat mutant developed by ethyl methanesulfonate (EMS) mutagenesis in a tetraploid Kronos WT variety (Kronos4652). A one base-pair alteration was located at the 496 site of *NPF2.12*, which causes a premature translational termination codon in the fourth exon that disrupts the full translation of the domain (Fig. 5a). We analyzed root growth and NO_3^- accumulation capacity in roots and shoots of the *npf2.12* mutant and WT under HN (10.0 mM) and LN (0.5 mM) NO_3^- treatments.

The *npf2.12* mutant plants demonstrated increased root growth performances under LN conditions than the WT after both 7- and 14 d of NO_3^- treatments (Fig. 5b,c). At HN availability, the WT plant exhibited increased root growth than the *npf2.12* mutant (Fig. 5b,c). Subsequently, a root phenotyping experiment revealed that root morphological traits, particularly TRL, RSA, and RV were significantly increased in the *npf2.12*

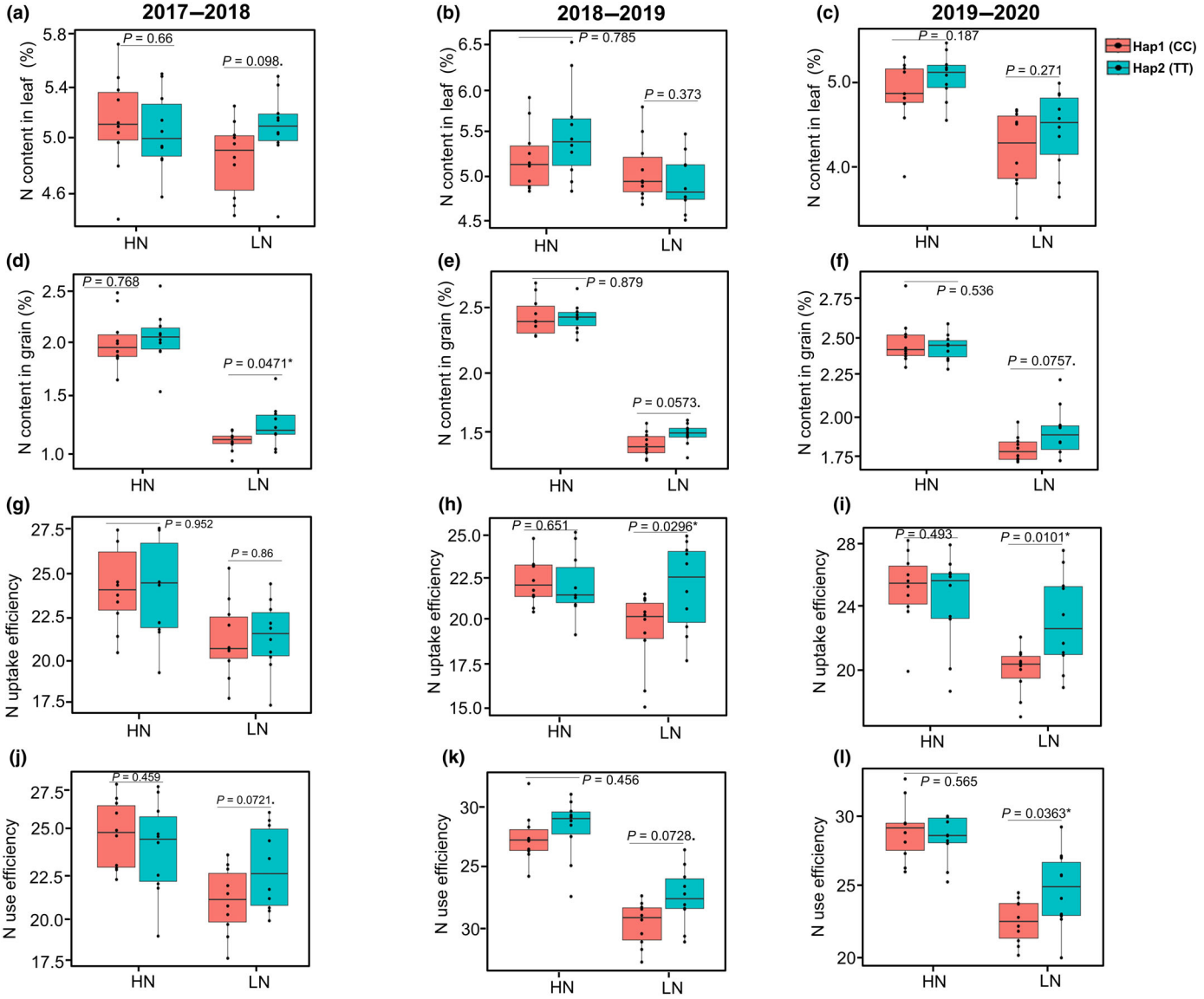

Fig. 4 Field-based evaluation of N-use efficiency related traits in wheat plants carrying TT and CC alleles of *TaNPF2.12* grown under high dose N (HN) (220 kg N ha^{-1}) and low dose N (LN) (0 kg N ha^{-1}) conditions in three growing seasons (2017–2018, 2018–2019, and 2019–2020). (a) N content in leaf (%) in 2017–2018; (b) N content in leaf in 2018–2019; (c) N content in leaf in 2019–2020; (d) N content in grain (%) in 2017–2018; (e) N content in grain in 2018–2019; (f) N content in grain in 2019–2020; (g) N uptake efficiency (ratio) in 2017–2018; (h) N uptake efficiency in 2018–2019; (i) N uptake efficiency in 2019–2020; (j) N use efficiency (ratio) in 2017–2018; (k) N use efficiency in 2018–2019; (l) N use efficiency in 2019–2020. The mean value was obtained from 10 cultivars of each allele from two independent plots as replication for each treatment. In boxplots, the horizontal line inside of the box represents the median, the whole box represents the interquartile range, the upper and lower whiskers represent scores outside the middle 50% and the black circles represents data points. Statistical significance was calculated based on one-way ANOVA: •, $P < 0.1$; *, $P < 0.05$.

mutant at LN than WT (Fig. 5d–f). These results implied that the WT allele functions as a negative regulator of important root morphological traits under LN conditions.

To estimate whether *NPF2.12* contributes to the divergence of NO_3^- uptake by root and transport to shoot, the mutant and WT seedlings were grown in a solution containing contrasting levels of NO_3^- (HN and LN). Under HN conditions, the NO_3^- content in shoots was decreased in mutant than in WT seedlings, while no significant differences between mutant and WT seedlings were observed with respect to NO_3^- content in roots. By contrast, under LN conditions, shoots of *npf2.12* plants displayed an increased NO_3^- content as compared to WT plants (Fig. 5h, i). Next, ^{15}N-label NO_3^- uptake and translocation analysis showed that *npf2.12* mutant seedlings had significantly higher

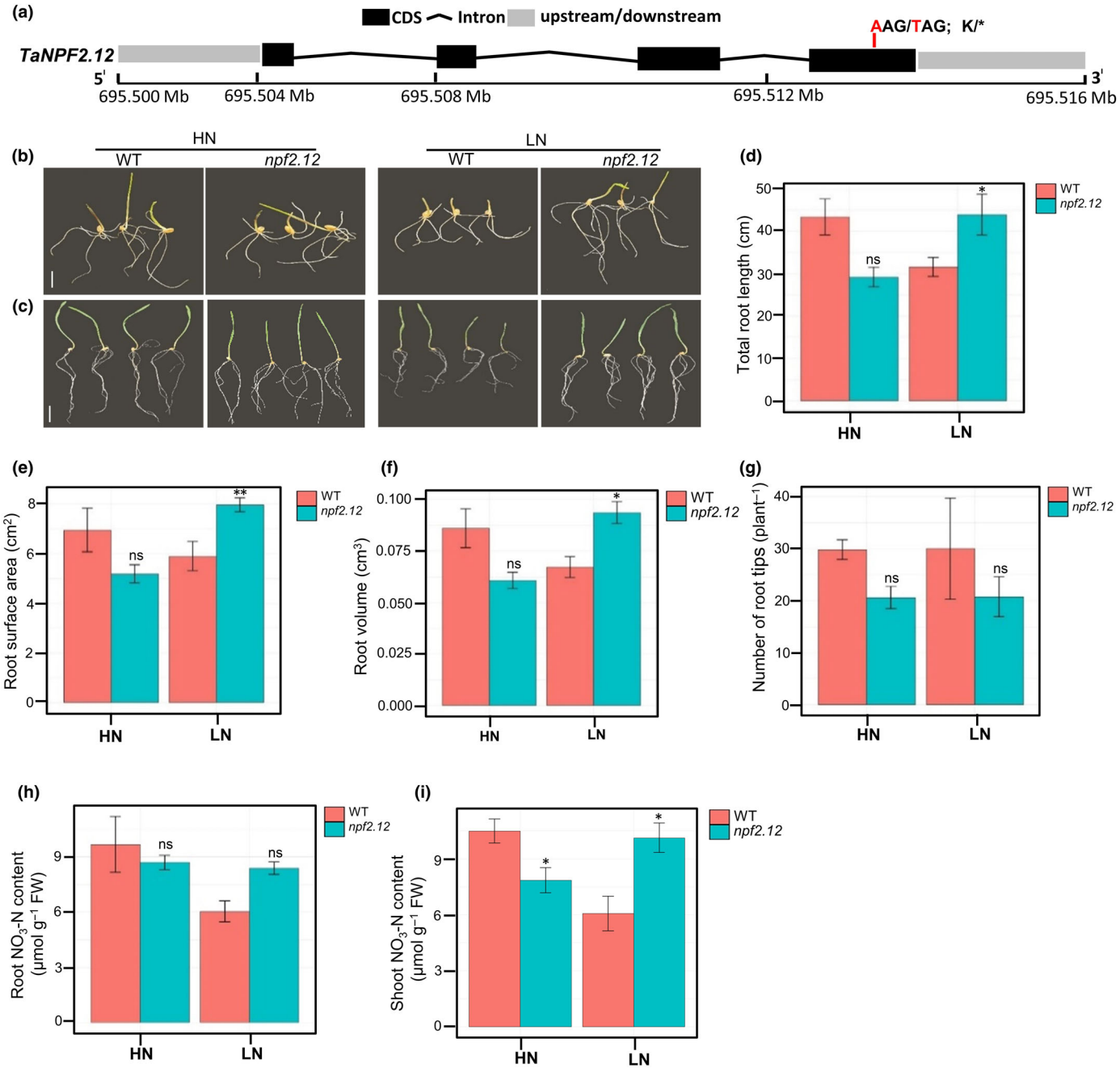

Fig. 5 Root phenotypes and NO_3^-–N content in root and shoot of *TaNPF2.12* EMS wheat mutant and wild-type (WT) under 10 mM (high dose N (HN)) and 0.5 mM NO_3^- (low dose N (LN)) conditions. (a) Gene structure of *TaNPF2.12* and mutant site. The red text indicates the SNP site; (b–g) phenotypic differences of root growth; (b) root growth phenotypes of *npf2.12* mutant and WT plants after 7-d exposure to NO_3^- treatments; (c) root growth phenotypes of *npf2.12* mutant and WT plants after 14-d exposure to NO_3^- treatments; (d) total root length; (e) root surface area; (f) root volume; (g) number of root tips; (h) NO_3^-–N content in roots and (i) NO_3^-–N content in shoots of mutant and WT plants grown at HN and LN availability. Bars represent mean ± SE (n = 06 independent biological replicates). Student's t-test: *, $P < 0.05$; **, $P < 0.01$; ***, $P < 0.001$ based on one-way ANOVA. Bars, 1 cm. NO, nitric oxide; ns, not significant.

^{15}N accumulation in roots and shoots compared with WT under LN conditions (Fig. 6a,b) as results of increased NO_3^- uptake and root-to-shoot transport activity compared with WT under LN (Fig. 6c,d). These findings are congruent with significant enhanced levels of N content measured in roots and shoots under LN supply (Fig. 6e,f). Taken together, these results suggest that under LN conditions, the *npf2.12* allele strongly influences root growth, accelerates NO_3^- uptake by roots, and increases NO_3^- translocation to aerial parts as compared to the *NPF2.12* WT allele.

Transcriptome analysis reveals differentially expressed genes involved in NO_3^- transport and assimilation between wild-type and *npf2.12* plants

To obtain insights into *NPF2.12* transcriptional responses and signaling pathways to NO_3^- availability, a comparative RNA-seq analysis was performed using WT and *npf2.12* mutant roots harvested after 14 d of HN and LN treatments. Differentially expressed genes (DEGs) between WT and *npf2.12* plants under two NO_3^- treatments were identified based on FDR adjusted *P*-value < 0.05 and a $\log_2$fold change threshold. RNA-seq analysis revealed a total of 106 914 DEGs, of which 826 genes were up-regulated in the WT (details in Methods S1; Fig. S5a–c). The mutant line was characterized by 255 and 345 up-regulated DEGs, while WT revealed 418 and 435 up-regulated genes in HN and LN, respectively (Table S18). Further analysis of DEGs identified the significant up-regulation of six NO_3^- transporter genes in WT in comparison with the mutant (HN to HN and LN to LN), five of these under HN conditions (Table S18). Contrastingly, only the member 5.5 of the NRT1 protein family was up-regulated in HN in the mutant plant when compared with WT ($P < 0.0001$, $\log_2$Fold = 6). However, a gene encoding a high-affinity NO_3^- transporter homolog and one encoding an NRT1 family protein (2.1) were up-regulated in WT compared with mutant under LN treatment (Table S19). Based on ShinyGO enrichment, nutrient transport pathways were found to be the most enriched pathways, followed by different biosynthetic or metabolic pathways (Fig. S6a,b). The NO_3^- transport and response pathways were the significantly enriched pathways in WT compared with the mutant under HN and a high-affinity NO_3^- transporter gene *NAR2.1* was involved in these pathways (Fig. 7a; Table S19). The NO biosynthesis and metabolic pathways were the most significant and enriched pathways found in *npf2.12* mutant compared with WT allele plants under LN treatment, where *NIA1* was specifically associated with

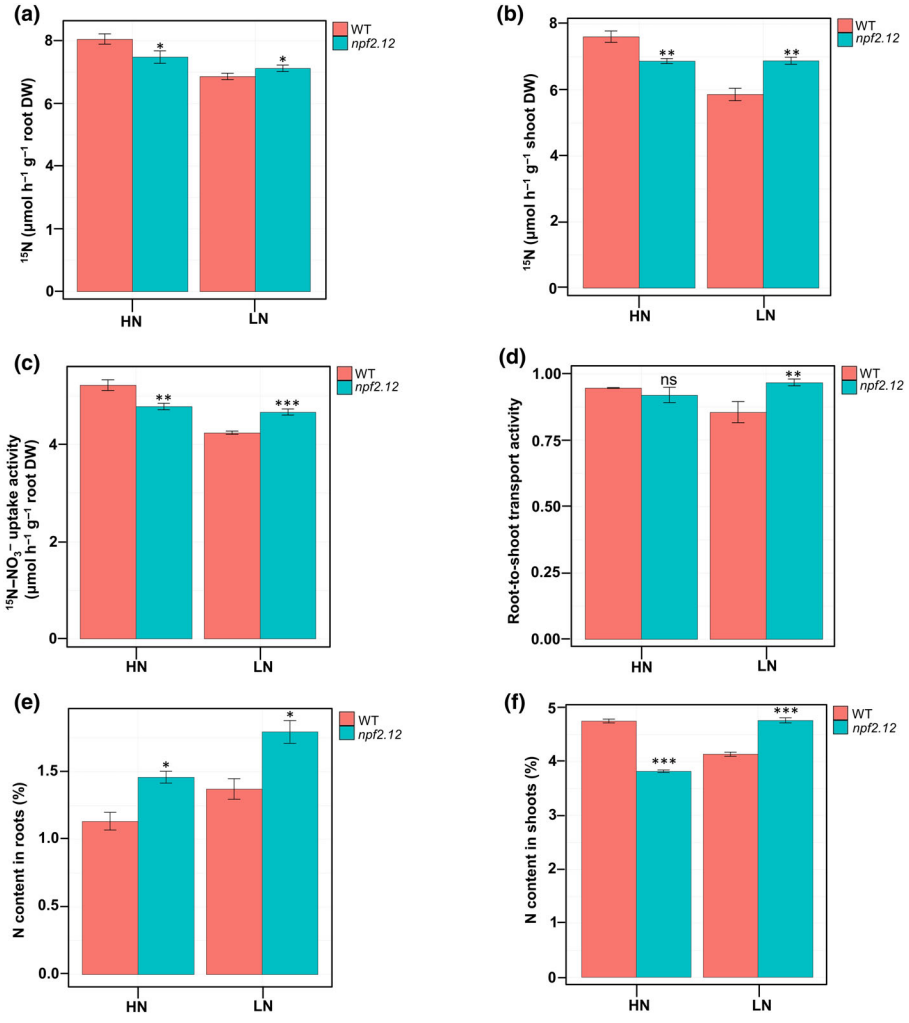

Fig. 6 NO_3^- uptake, translocation and total N accumulation capacities of *TaNPF2.12* wild-type (WT) plants and *npf2.12* mutant plants. (a) ^{15}N–NO_3^- accumulation in roots; (b) ^{15}N–NO_3^- accumulation in shoots; (c) ^{15}N–NO_3^- uptake activity; (d) root-to-shoot transport capacity of WT and *npf2.12* mutant seedlings exposed to either 5 mM (HN) or 0.5 mM KNO_3 (LN) ^{15}N-labeled KNO_3 for 3 h; (e) N content in roots and (f) N content in shoots under 10 mM (high dose N (HN)) and 0.5 mM NO_3^- (low dose N (LN)) availability. Bars represent mean ± SE ($n = 03$ independent biological replicates). Student's *t*-test: *, $P < 0.05$; **, $P < 0.01$; ***, $P < 0.001$ based on one-way ANOVA. NO, nitric oxide; ns, not significant.

these pathways (Fig. 7b; Table S19). Hence, we further hypothesize that *NIA1* regulates NO production underlying activities of NR in *npf2.12* mutant plants that might be responsible to modulate root growth and NO_3^- transport to the shoot under LN supply.

Next, to gain an overview of *NIA1*-dependent NO biosynthesis under NO_3^- availability, we compared *NIA1* expression, activities of NR, and NO production capacity between WT and *npf2.12* mutant plants. *NIA1* transcript levels were significantly ($P < 0.001$) increased in mutant plants in response to LN than in WT (Fig. 7c). Accordingly, under LN treatment, *npf2.12* mutant plants showed significantly higher NR activities and NO production levels in roots than the WT, while no significant changes in NR activities were observed in shoots under both HN and LN concentrations (Fig. 7d–f). Together, these results indicate that upon LN inputs, when the *NPF2.12* allele is repressed, the *NIA1* transcription is highly activated to confer NR-mediated NO production, which might be critical for root growth, NO_3^- uptake, and root-to-shoot transport (Fig. 8).

Discussion

The trait values observed for all of the root traits in both wheat and barley were significantly reduced by HN supply, which is an agreement with previous reports (P. Li *et al.*, 2015, Y. Li *et al.*, 2015; Xin *et al.*, 2021). For 21 root traits in wheat and nine in barley, the GWAS identified 70 and 43 SNPs that are in proximity of 341 and 38 candidate genes related to N responses and root growth across wheat and barley chromosomes, respectively. Using a comparative GWAS between wheat and barley, three ORFs (open reading frames) of convergently selected genes were identified, which include two paralogs in wheat annotated as NO_3^- transporter homologous genes *TraesCS3B02G454000* and *TraesCS3B02G454100 (TaNPF2.12)* and one in barley *HORVU3Hr1G092870* (*HvNPF2.12*) on chromosome 3. The closest homolog in Arabidopsis encodes *AtNRT1.6*, a known low-affinity NO_3^- transporter (Almagro *et al.*, 2008). Within two homologues in wheat, we considered only *TraesCS3B02G454000* for detailed investigation in this study, whereas the function of the other homolog needs to be investigated in further studies. Nevertheless, further studies are needed to analyze the function of the other paralogs in wheat and homologues between wheat and barley. This is because the annotation of two additional candidate genes besides *NPF2.12* suggests their involvement in auxin and abscisic acid signaling pathways and, thus, they might be also associated with root phenotypes under low N conditions as suggested by work in Arabidopsis (Jia *et al.*, 2021; Liu & von Wirén, 2022).

In previous studies, several NO_3^- transporter NPF genes have been reported in hexaploid wheat and barley, which are mainly located on chromosome 3 (Guo *et al.*, 2020; Wang *et al.*, 2020). In agreement with this, the comparative GWAS provided a conserved synteny on chromosomes 3 of wheat and barley by revealing a high number of candidate genes related to NUE. Next, protein sequence analysis revealed a conserved domain of MFS in both *TaNPF2.12* and *HvNPF2.12*. It has been well-documented that NPF proteins belong to a much larger MFS of secondary active transporters (Newstead *et al.*, 2011; Reddy *et al.*, 2012) that utilize chemiosmotic ion gradients to facilitate substrate transport into the cell (Fei *et al.*, 1994; Chiang *et al.*, 2004) and that this family comprises both low-affinity NO_3^- and peptide transporters sharing high sequence homology (Tsay *et al.*, 2007; Léran *et al.*, 2014). Recently, genetic modification of an NO_3^- assimilation gene *OsNR2* encoding NR activity was shown to result in an enhancement of NUE in rice (Yu *et al.*, 2021). Furthermore, the NPF NO_3^- transporter *OsNPF6.1* varies in both protein and promoter sequences, and its rare natural allele enhances NUE under field trials in rice (Tang *et al.*, 2019).

Sequence analysis of the coding and promoter elements of this gene of 40 wheat and 40 barley NO_3^- contrasting genotypes demonstrated that only the promoter region of *TaNPF2.12* and *HvNPF2.12* had consistent allelic variations among diverse wheat but also barley genotypes. The results implied that the majority of tolerant genotypes, that is, with higher RV and TRL belong to Hap2, while most of the sensitive genotypes, that is, lower RV and TRL under LN/HN conditions belong to Hap1. Consistently, root phenotyping and NO_3^- determination also indicated that the Hap2 promoters of *TaNPF2.12* and *HvNPF2.12* were significantly associated with better root growth, NO_3^- uptake, and translocation capacity than Hap1 under LN (0.5 mM NO_3^-). Importantly, elite *NPF2.12* alleles in both wheat and barley showed constantly reduced expression under LN conditions (Figs 2c, 3c). These data suggest that inactivation of the *NPF2.12* promoter in Hap2 under LN might result in better root growth, NO_3^- uptake and root-to-shoot transport capacity. Furthermore, we assume that decreased expression levels of *TaNPF2.12* at LN supply may also affect NUpE and NUE. This work illustrates that reduced levels of $TaNPF2.12^{TT}$ transcript led to increased accumulation of N in leaves and grains, resulting in improved NUpE and NUE at LN supply compared to plants harboring the $TaNPF2.12^{CC}$ allele. Thus, in contrast to the studies on *OsNPF6.1* where a rare natural allele is induced under LN conditions causing increased NUE (Tang *et al.*, 2019), the identified elite Hap2 allele $NPF2.12^{TT}$ causes increased NUpE and NUE by deactivation of the candidate NO_3^- transceptor homolog under LN.

To verify our hypothesis that loss of NPF2.12 function might contribute to root growth and NO_3^- transport capacity, an *npf2.12* EMS mutant was used to perform a series of phenotypical and physiological experiments including a comparative transcriptome analysis. Root phenotyping under contrasting NO_3^- input levels showed that the TRL, RSA, and RV of mutant plants were significantly higher than that of the WT at LN concentration, indicating that the mutant allele contributes to a better root growth. A ^{15}N–NO_3^- uptake and translocation assay demonstrated an increase in ^{15}N accumulation in roots and shoots, in NO_3^- uptake by roots and in transport activity from roots to shoots in *npf2.12* seedlings as compared to WT seedlings under LN conditions indicating that the WT allele is indeed a negative regulator of NO_3^- uptake and transport from root-to-shoot. Remarkably, *npf2.12* plants displayed less NO_3^- content in shoots, ^{15}N content in both roots and shoots, ^{15}N–NO_3 uptake activity and N content in shoots (Figs 5j, 6a–c,f) under HN conditions, suggesting that under HN conditions, NPF2.12 appears to be a positive regulator of N-acquisition. Something similar, albeit in a different tissue, has been reported in Arabidopsis: *nrt1.6–3*

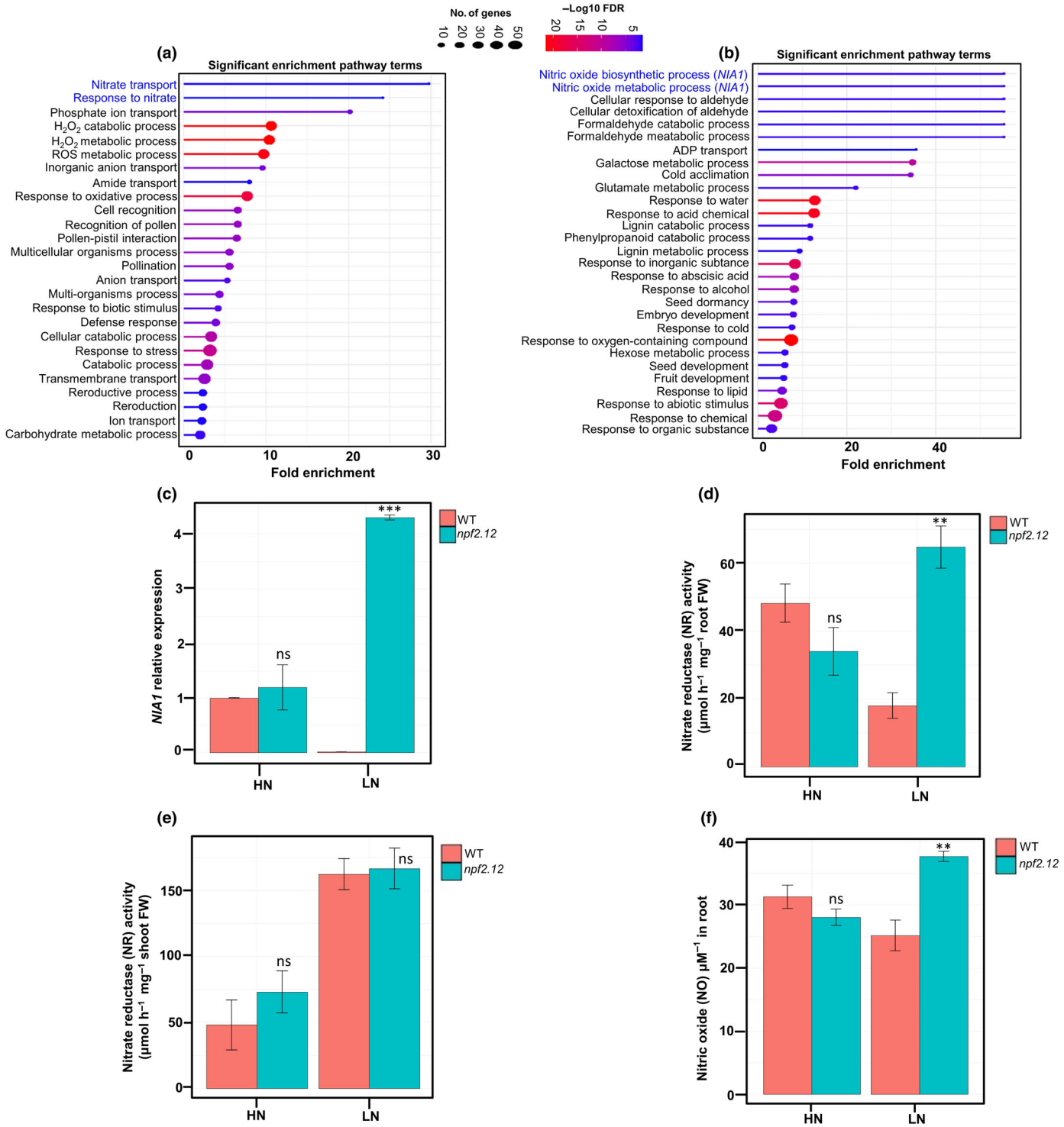

Fig. 7 RNA sequencing, *NIA1* expression, nitrate reductase (NR) activity, and nitric oxide (NO) content analyses of the *TaNPF2.12* wild-type (WT) and mutant allele after 14-d exposed to high dose N (HN) (10 mM) and low dose N (LN) (0.5 mM NO_3^-). (a) Gene ontology and the 26 most significantly enriched pathways in WT compared to mutant allele under HN treatment; (b) gene ontology and the 29 most significantly enriched pathways in *npf2.12* mutant compared to WT allele under LN treatment analyzed by ShinyGO enrichment tool; (c) comparison of transcript expression levels of *NIA1* by qRT-PCR; (d) NR activity in roots; (e) NR activity in shoots and (f) NO contents in roots between WT and mutant plants. We considered differentially expressed genes (DEGs) when on average more than two normalized reads across all three replicates were recognized. Bars represent mean ± SE (n = 06 independent biological replicates). Student's t-test: *, $P < 0.05$; **, $P < 0.01$; ***, $P < 0.001$ based on one-way ANOVA. ns, not significant.

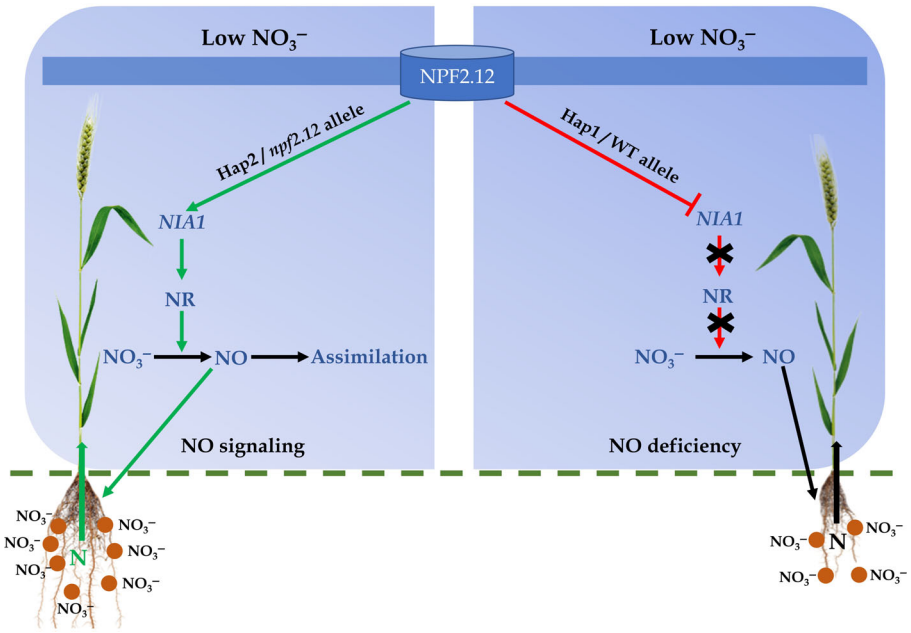

Fig. 8 Depiction of a proposed model of the regulatory pathways of *TaNPF2.12* in response to low dose N (LN) (0.5 mM NO_3^-) availability. The haplotype 2 (Hap2) allele (similarly the *npf2.12* mutant allele carrying a premature termination codon in the fourth exon) as a consequence of failing to allow proper sensing low levels of N, causes upregulation of *NIA1* transcript levels resulting in the elicitation of NR activity and ultimately NO production. Consequent NO signaling leads to enhanced root growth traits that enable to increased levels NO_3^- acquisition (pathway on the left) and finally increased amounts of N in the entire plant. Further, we hypothesise that the Hap2 allele is more efficient under low N conditions (pathway on the left). By contrast, the Hap1 or wild-type (WT) allele suppresses *NIA1* transcripts levels causing inhibition of NR activity and NO production in response to LN availability. These reduced levels of NO are associated with stunted root growth and decreased NO_3^- acquisition (pathway on the right). The green arrows indicates the upregulation and the red with blunt ended arrow indicate down regulation of the gene. The black arrows indicates reaction flow. The green and black upstraight arrows indicates increased and decreased NO_3^- root-to-shoot transport, respectively. The brown colour circles indicate NO_3^-. *NIA1*, *NITRATE REDUCTASE 1*; NR, nitrate reductase; NO, nitric oxide. Wheat plant image source: SeekPNG.com.

mutant plants defective in the low-affinity NO_3^- transporter NRT1.6 display strong seed abortion phenotypes under regular and under HN conditions (Almagro *et al.*, 2008). By contrast, under LN conditions, seed abortion defects increased in Col-0, that is, plants carrying the WT *NRT1.6* allele, but decreased in *nrt1.6–3* mutant plants (Almagro *et al.*, 2008) suggesting that NRT1.6 similar to NPF2.12 might have different activities with distinct physiological consequences under HN and LN conditions. We speculate that such different activities might relate to a potential function of these proteins as transceptors as has been proposed for Arabidopsis NRT1.1 (Gojon *et al.*, 2011; Bouguyon *et al.*, 2015). Under HN conditions, WT plants carrying the *NPF2.12* allele show increased NO_3^- accumulation due to the low-affinity NO_3^- uptake activity of *NPF2.12* (Fig. 5i). The situation with the wheat and barley elite haplotypes is obviously more complex than loss-of-functions mutants since their expression is increased under HN conditions (Figs 2c, 3c). In this scenario, compromised *NPF2.12*-dependent NO_3^- sensing in *npf2.12* plants or in plants carrying the elite Hap2 allele (TT) triggers *NIA1* expression and NO production and thereby induces morphological traits in roots under low N conditions. Increased root length, root surface area, and root volume are correlates with higher levels of NO_3^- acquisition that ultimately leads to increase NO_3^- root-to-shoot transport activity under low N conditions (Fig. 8).

Our comparative transcriptome analysis found indeed that *NIA1* transcript levels highly increased in the presence of the *npf2.12* mutant allele when compared to the WT allele in LN conditions. Increased *NIA1* levels are likely responsible for increased NR activity and NO production. It has been well-established that the NR-defective *nia1* mutant displays reduced levels of endogenous NO (Zhao *et al.*, 2009). When plant sense NO_3^-, multiple NO_3^- assimilation pathway genes, importantly *NIA*, are induced within minutes to serve as NO_3^- enhancer (Wang *et al.*, 2010). NR is a key enzyme involved in the first step of NO_3^- assimilation, encoded by two genes, *NIA1* and *NIA2* (Wilkinson & Crawford, 1993), and *NIA1* is a major constituent underlying NR-dependent NO production (Zhao *et al.*, 2009), which contributes to better root growth, NO_3^- uptake by roots and transport to shoots (Neill *et al.*, 2003; Sun *et al.*, 2015). Therefore, the identified *NPF2.12* may be part of a regulatory network, able to induce *NIA1* transcript encoding NR activity, thus resulting in elevated NO production to stimulate root growth, NO_3^- uptake, and transport activity and subsequently to increase high-NUE under LN conditions.

In summary, we identified elite alleles of a candidate NO_3^- transceptor *NPF2.12* that are convergently selected in wheat and barley and a presumptive role of these alleles in activating *NIA1* expression, NR-mediated NO biosynthesis to stimulate root growth and root-to-shoot NO_3^- translocation under limited N availability. It is therefore critically important to exploit natural allelic variants of *NPF2.12*, or to develop *de novo* variants by genome editing to enable breeders to utilize this gene in breeding programs. This study also highlights that the genetic control of

NPF2.1-NIA1 interactions might represent an obvious potential strategy towards the breeding of high-NUE cereal varieties. Further efforts focusing on the in-depth transport activity, subcellular localization, tissue-specific expression, and regulatory networks of *NPF2.12* with other convergent orthologs across cereal species could largely accelerate breeding of improved NUE.

Acknowledgements

This research was supported from the German Federal Ministry of Education and Research (BMBF) project Breeding Innovations in Wheat for Resilient Cropping Systems (BRIWECS) funded with the grant 031A354 and for support of the Federal Office for Agriculture and Food project 'POeWER' (FKZ: 2818105815). AB and GS acknowledges funding from the Deutsche Forschungsgemeinschaft under Germany's Excellence Strategy – EXC 2070 – 390732324 (PhenoRob). MNS acknowledges financial support from the German Academic Exchange Service (DAAD with ref no. 91690550). The authors thank Mohammad Kamruzzaman, Marissa B. Barbosa, Patrice Koua, Said Dadshani and Karin Woitol for their help during root harvesting under field experiments. The authors extend acknowledgement to the campus Klein-Altendorf staff for taking care of field experiments. Also grateful to the International Center for Agricultural Research in the Dry Areas (ICARDA), Rabat for providing us the barley association panel. The authors also thank Deborah Rupprecht and Marília Kamleitner, INRES-Plant Nutrition, University of Bonn for their great support during ^{15}N analysis and manuscript correction, respectively. Also acknowledge to NGC core facility by Medical Faculty at University of Bonn. Open Access funding enabled and organized by Projekt DEAL.

Competing interests

None declared.

Author contributions

JL and AB designed and supervised the experiments. MNS, KP and SKB performed root phenotyping and molecular analysis and also performed phenotypic data and GWAS analysis. MNS and BSadeqi performed field experiments. MS and BStich performed transcriptome data analysis. MS-G provided barley materials and genotyping data. GS supported ^{15}N analysis. MNS prepared the manuscript draft. MNS, BStich, GS, JL and AB edited and revised the manuscript. All authors read and approved the final version of the manuscript.

ORCID

Agim Ballvora https://orcid.org/0000-0003-0949-8311
Gabriel Schaaf https://orcid.org/0000-0001-9022-4515
Md. Nurealam Siddiqui https://orcid.org/0000-0003-4604-3471
Benjamin Stich https://orcid.org/0000-0001-6791-8068

Data availability

The data of this study are available in the supporting information or from the corresponding authors upon request.

References

Alaux M, Rogers J, Letellier T, Flores R, Alfama F, Pommier C, Mohellibi N, Durand S, Kimmel E, Michotey C *et al.* 2018. Linking the International Wheat Genome Sequencing Consortium bread wheat reference genome sequence to wheat genetic and phenomic data. *Genome Biology* **19**: 111.

Almagro A, Lin SH, Tsay YF. 2008. Characterization of the Arabidopsis nitrate transporter NRT1.6 reveals a role of nitrate in early embryo development. *Plant Cell* **20**: 3289–3299.

Alvarez JM, Vidal EA, Gutiérrez RA. 2012. Integration of local and systemic signaling pathways for plant N responses. *Current Opinion in Plant Biology* **15**: 185–191.

Amezrou R, Gyawali S, Belqadi L, Chao S, Arbaoui M, Mamidi S, Rehman S, Sreedasyam A, Verma RPS. 2018. Molecular and phenotypic diversity of ICARDA spring barley (*Hordeum vulgare* L.) collection. *Genetic Resources and Crop Evolution* **65**: 255–269.

Bagchi R, Salehin M, Adeyemo OS, Salazar C, Shulaev V, Sherrier DJ, Dickstein R. 2012. Functional assessment of the *Medicago truncatula* NIP/LATD protein demonstrates that it is a high-affinity nitrate transporter. *Plant Physiology* **160**: 906–916.

Bayer MM, Rapazote-Flores P, Ganal M, Hedley PE, Macaulay M, Plieske J, Ramsay L, Russell J, Shaw PD, Thomas W *et al.* 2017. Development and evaluation of a barley 50k iSelect SNP array. *Frontiers in Plant Science* **8**: 1792.

Begum H, Alam MS, Feng Y, Koua P, Ashrafuzzaman M, Shrestha A, Kamruzzaman M, Dadshani S, Ballvora A, Naz AA *et al.* 2020. Genetic dissection of bread wheat diversity and identification of adaptive loci in response to elevated tropospheric ozone. *Plant, Cell & Environment* **43**: 2650–2665.

Bouguyon E, Brun F, Meynard D, Kubeš M, Pervent M, Leran S, Lacombe B, Krouk G, Guiderdoni E, Zažímalová E *et al.* 2015. Multiple mechanisms of nitrate sensing by Arabidopsis nitrate transceptor NRT1.1. *Nature Plants* **1**: 1–8.

Brenchley WE, Jackson VG. 1921. Root development in barley and wheat under different conditions of growth. *Annals of Botany* **35**: 533–556.

Cataldo DA, Maroon M, Schrader LE, Youngs VL. 1975. Rapid colorimetric determination of nitrate in plant tissue by nitration of salicylic acid. *Communications in Soil Science and Plant Analysis* **6**: 71–80.

Chen KE, Chen HY, Tseng CS, Tsay YF. 2020. Improving nitrogen use efficiency by manipulating nitrate remobilization in plants. *Nature Plants* **6**: 1126–1135.

Chen X, Cui Z, Fan M, Vitousek P, Zhao M, Ma W, Wang Z, Zhang W, Yan X, Yang J *et al.* 2014. Producing more grain with lower environmental costs. *Nature* **514**: 486–489.

Chiang C-S, Stacey G, Tsay Y-F. 2004. Mechanisms and functional properties of two peptide transporters, AtPTR2 and fPTR2. *Journal of Biological Chemistry* **279**: 30150–30157.

Dadshani S, Mathew B, Ballvora A, Mason AS, Léon J. 2021. Detection of breeding signatures in wheat using a linkage disequilibrium-corrected mapping approach. *Scientific Reports* **11**: 5527.

Davidson RM, Gowda M, Moghe G, Lin H, Vaillancourt B, Shiu S-H, Jiang N, Robin BC. 2012. Comparative transcriptomics of three Poaceae species reveals patterns of gene expression evolution. *The Plant Journal* **71**: 492–502.

Devos KM, Gale MD. 1997. Comparative genetics in the grasses. *Plant Molecular Biology* **35**: 3–15.

Dhital S, Raun WR. 2016. Variability in optimum nitrogen rates for maize. *Agronomy Journal* **108**: 2165–2173.

Fan X, Naz M, Fan X, Xuan W, Miller AJ, Xu G. 2017. Plant nitrate transporters: from gene function to application. *Journal of Experimental Botany* **68**: 2463–2475.

Fei YJ, Kanai Y, Nussberger S, Ganapathy V, Leibach FH, Romero MF, Singh SK, Boron WF, Hediger MA. 1994. Expression cloning of a mammalian proton-coupled oligopeptide transporter. *Nature* **368**: 563–566.

Foley JA, Ramankutty N, Brauman KA, Cassidy ES, Gerber JS, Johnston M, Mueller ND, O'Connell C, Ray DK, West PC *et al.* 2011. Solutions for a cultivated planet. *Nature* **478**: 337–342.

Garnett T, Appleby MC, Balmford A, Bateman IJ, Benton TG, Bloomer P, Burlingame B, Dawkins M, Dolan L, Fraser D *et al.* 2013. Sustainable intensification in agriculture: premises and policies. *Science* **341**: 33–34.

Gibbon D, Dixon J, Flores Velazquez D. 2007. *Beyond drought tolerant maize: study of additional priorities in maize*. Report to Generation Challenge Program. Mexico: CIMMYT. [WWW document] URL http://hdl.handle.net/10883/818 [accessed 10 February 2022].

Gojon A, Krouk G, Perrine-Walker F, Laugier E. 2011. Nitrate transceptor(s) in plants. *Journal of Experimental Botany* **62**: 2299–2308.

Guo B, Li Y, Wang S, Li D, Lv C, Xu R. 2020. Characterization of the nitrate transporter gene family and functional identification of HvNRT2.1 in barley (*Hordeum vulgare* L.). *PLoS ONE* **15**: e0232056.

Hirel B, Tétu T, Lea PJ, Dubois F. 2011. Improving nitrogen use efficiency in crops for sustainable agriculture. *Sustainability* **3**: 1452–1485.

Hu B, Wang W, Ou S, Tang J, Li H, Che R, Zhang Z, Chai X, Wang H, Wang Y *et al.* 2015. Variation in NRT1.1B contributes to nitrate-use divergence between rice subspecies. *Nature Genetics* **47**: 834–838.

IBGC. 2012. International Barley Genome Sequencing Consortium: A physical, genetic and functional sequence assembly of the barley genome. *Nature* **491**: 711.

Jia Z, Giehl RF, von Wirén N. 2021. Local auxin biosynthesis acts downstream of brassinosteroids to trigger root foraging for nitrogen. *Nature Communications* **12**: 1–12.

Jia Z, Giehl RFH, Meyer RC, Altmann T, von Wirén N. 2019. Natural variation of BSK3 tunes brassinosteroid signaling to regulate root foraging under low nitrogen. *Nature Communications* **10**: 2378.

Johnson HW, Robinson HF, Comstock RE. 1955. Genotypic and phenotypic correlations in soybeans and their implications in selection1. *Agronomy Journal* **47**: 477–483.

Kadam NN, Tamilselvan A, Lawas LMF, Quinones C, Bahuguna RN, Thomson MJ, Dingkuhn M, Muthurajan R, Struik PC, Yin X *et al.* 2017. Genetic control of plasticity in root morphology and anatomy of rice in response to water deficit. *Plant Physiology* **174**: 2302–2315.

Kadam NN, Yin X, Bindraban PS, Struik PC, Jagadish KSV. 2015. Does morphological and anatomical plasticity during the vegetative stage make wheat more tolerant of water deficit stress than rice? *Plant Physiology* **167**: 1389–1401.

Kang HM, Sul JH, Service SK, Zaitlen NA, Kong S, Freimer NB, Sabatti C, Eskin E. 2010. Variance component model to account for sample structure in genome-wide association studies. *Nature Genetics* **42**: 348–354.

Klein SP, Reeger JE, Kaeppler SM, Brown KM, Lynch JP. 2020. Shared genetic architecture underlying root metaxylem phenotypes under drought stress in cereals. *bioRxiv*. doi: 10.1101/2020.11.02.365247.

Koua AP, Oyiga BC, Baig MM, Léon J, Ballvora A. 2021. Breeding driven enrichment of genetic variation for key yield components and grain starch content under drought stress in winter wheat. *Frontiers in Plant Science* **12**: 684205.

Krasileva KV, Vasquez-Gross HA, Howell T, Bailey P, Paraiso F, Clissold L, Simmonds J, Ramirez-Gonzalez RH, Wang X, Borrill P *et al.* 2017. Uncovering hidden variation in polyploid wheat. *Proceedings of the National Academy of Sciences, USA* **114**: E913–E921.

Krouk G, Crawford NM, Coruzzi GM, Tsay Y-F. 2010. Nitrate signaling: adaptation to fluctuating environments. *Current Opinion in Plant Biology* **13**: 266–273.

Larkin MA, Blackshields G, Brown NP, Chenna R, McGettigan PA, McWilliam H, Valentin F, Wallace IM, Wilm A, Lopez R *et al.* 2007. ClustalW and ClustalX v.2.0. *Bioinformatics* **23**: 2947–2948.

Lebender U, Senbayram M, Lammel J, Kuhlmann H. 2014. Effect of mineral nitrogen fertilizer forms on N_2O emissions from arable soils in winter wheat production. *Journal of Plant Nutrition and Soil Science* **177**: 722–732.

Léran S, Varala K, Boyer J-C, Chiurazzi M, Crawford N, Daniel-Vedele F, David L, Dickstein R, Fernandez E, Forde B *et al.* 2014. A unified nomenclature of NITRATE TRANSPORTER 1/PEPTIDE TRANSPORTER family members in plants. *Trends in Plant Science* **19**: 5–9.

Li L, Guo N, Niu J, Wang Z, Cui X, Sun J, Zhao T, Xing H. 2016. Loci and candidate gene identification for resistance to *Phytophthora sojae* via association analysis in soybean (*Glycine max* (L.) Merr.). *Molecular Genetics and Genomics* **291**: 1095–1103.

Li P, Chen F, Cai H, Liu J, Pan Q, Liu Z, Gu R, Mi G, Zhang F, Yuan L. 2015. A genetic relationship between nitrogen use efficiency and seedling root traits in maize as revealed by QTL analysis. *Journal of Experimental Botany* **66**: 3175–3188.

Li Y, Ouyang J, Wang Y-Y, Hu R, Xia K, Duan J, Wang Y, Tsay Y-F, Zhang M. 2015. Disruption of the rice nitrate transporter OsNPF2.2 hinders root-to-shoot nitrate transport and vascular development. *Scientific Reports* **5**: 9635.

Ligero F, Lluch C, Hervas A, Olivares J, Bedmar EJ. 1987. Effect of nodulation on the expression of nitrate reductase activity in pea cultivars. *New Phytologist* **107**: 53–61.

Liu K-H, Tsay Y-F. 2003. Switching between the two actions modes of the dual-affinity nitrate transporter CHL1 by phosphorylation. *EMBO Journal* **22**: 1005–1013.

Liu LH, Ludewig U, Frommer WB, von Wirén N. 2003. AtDUR3 encodes a new type of high-affinity urea/H^+ symporter in Arabidopsis. *Plant Cell* **15**: 790–800.

Liu Y, Hu B, Chu C. 2016. ^{15}N-nitrate uptake activity and root-to-shoot transport assay in rice. *Bio-Protocol* **6**: e1897.

Liu Y, von Wirén N. 2022. Integration of nutrient and water availabilities via auxin into the root developmental program. *Current Opinion in Plant Biology* **65**: 102117.

Mahmud K, Panday D, Mergoum A, Missaoui A. 2021. Nitrogen losses and potential mitigation strategies for a sustainable agroecosystem. *Sustainability* **13**: 2400.

Miller AJ, Fan X, Orsel M, Smith SJ, Wells DM. 2007. Nitrate transport and signalling. *Journal of Experimental Botany* **58**: 2297–2306.

Moll RH, Kamprath EJ, Jackson WA. 1982. Analysis and interpretation of factors which contribute to efficiency of nitrogen utilization. *Agronomy Journal* **74**: 562–564.

Morère-Le Paven M-C, Viau L, Hamon A, Vandecasteele C, Pellizzaro A, Bourdin C, Laffont C, Lapied B, Lepetit M, Frugier F *et al.* 2011. Characterization of a dual-affinity nitrate transporter MtNRT1.3 in the model legume *Medicago truncatula*. *Journal of Experimental Botany* **62**: 5595–5605.

Muzammil S, Shrestha A, Dadshani S, Pillen K, Siddique S, Léon J, Naz AA. 2018. An ancestral allele of pyrroline-5-carboxylate synthase1 promotes proline accumulation and drought adaptation in cultivated barley. *Plant Physiology* **178**: 771–782.

Neill SJ, Desikan R, Hancock JT. 2003. Nitric oxide signalling in plants. *New Phytologist* **159**: 11–35.

Newstead S, Drew D, Cameron AD, Postis VLG, Xia X, Fowler PW, Ingram JC, Carpenter EP, Sansom MSP, McPherson MJ *et al.* 2011. Crystal structure of a prokaryotic homologue of the mammalian oligopeptide-proton symporters, PepT1 and PepT2. *EMBO Journal* **30**: 417–426.

O'Brien JA, Vega A, Bouguyon E, Krouk G, Gojon A, Coruzzi G, Gutiérrez RA. 2016. Nitrate transport, sensing, and responses in plants. *Molecular Plant* **9**: 837–856.

Oyiga BC, Palczak J, Wojciechowski T, Lynch JP, Naz AA, Léon J, Ballvora A. 2020. Genetic components of root architecture and anatomy adjustments to water-deficit stress in spring barley. *Plant, Cell & Environment* **43**: 692–711.

R Core Team. 2013. *R: a language and environment for statistical computing*. Vienna, Austria: R Foundation for Statistical Computing. [WWW document] URL http://www.R-project.org/ [accessed 1 November 2021].

Reddy VS, Shlykov MA, Castillo R, Sun EI, Saier MH. 2012. The major facilitator superfamily (MFS) revisited. *FEBS Journal* **279**: 2022–2035.

Salse J, Abrouk M, Murat F, Quraishi UM, Feuillet C. 2009. Improved criteria and comparative genomics tool provide new insights into grass paleogenomics. *Briefings in Bioinformatics* **10**: 619–630.

Schneider CA, Rasband WS, Eliceiri KW. 2012. NIH image to ImageJ: 25 yr of image analysis. *Nature Methods* **9**: 671–675.

Schreiber AW, Sutton T, Caldo RA, Kalashyan E, Lovell B, Mayo G, Muehlbauer GJ, Druka A, Waugh R, Wise RP *et al.* 2009. Comparative transcriptomics in the Triticeae. *BMC Genomics* **10**: 285.

Siddiqi MY, Glass AD, Ruth TJ, Rufty TW. 1990. Studies of the uptake of nitrate in barley: I. Kinetics of $^{13}NO_3^-$ influx. *Plant Physiology* **93**: 1426–1432.

Siddiqui MN, Léon J, Naz AA, Ballvora A. 2021b. Genetics and genomics of root system variation in adaptation to drought stress in cereal crops. *Journal of Experimental Botany* **72**: 1007–1019.

Siddiqui MN, Teferi TJ, Ambaw AM, Gabi MT, Koua P, Léon J, Ballvora A. 2021a. New drought-adaptive loci underlying candidate genes on wheat chromosome 4B with improved photosynthesis and yield responses. *Physiologia Plantarum* **173**: 2166–2180.

Stich B, Möhring J, Piepho H-P, Heckenberger M, Buckler ES, Melchinger AE. 2008. Comparison of mixed-model approaches for association mapping. *Genetics* **178**: 1745–1754.

Storey JD, Bass AJ, Dabney A, Robinson D, Warnes G. 2020. *qvalue: Q-value estimation for false discovery rate control*. R package v.2.22.0. [WWW document] URL http://github.com/jdstorey/qvalue [accessed 8 November 2020].

Sun H, Li J, Song W, Tao J, Huang S, Chen S, Hou M, Xu G, Zhang Y. 2015. Nitric oxide generated by nitrate reductase increases nitrogen uptake capacity by inducing lateral root formation and inorganic nitrogen uptake under partial nitrate nutrition in rice. *Journal of Experimental Botany* **66**: 2449–2459.

Tang W, Ye J, Yao X, Zhao P, Xuan W, Tian Y, Zhang Y, Xu S, An H, Chen G *et al.* 2019. Genome-wide associated study identifies NAC42-activated nitrate transporter conferring high nitrogen use efficiency in rice. *Nature Communications* **10**: 5279.

Trachsel S, Kaeppler SM, Brown KM, Lynch JP. 2011. Shovelomics: high throughput phenotyping of maize (*Zea mays* L.) root architecture in the field. *Plant and Soil* **341**: 75–87.

Tsay Y-F, Chiu C-C, Tsai C-B, Ho C-H, Hsu P-K. 2007. Nitrate transporters and peptide transporters. *FEBS Letters* **581**: 2290–2300.

Tsay YF, Schroeder JI, Feldmann KA, Crawford NM. 1993. The herbicide sensitivity gene CHL1 of Arabidopsis encodes a nitrate-inducible nitrate transporter. *Cell* **72**: 705–713.

Vidal EA, Gutiérrez RA. 2008. A systems view of nitrogen nutrient and metabolite responses in Arabidopsis. *Current Opinion in Plant Biology* **11**: 521–529.

Vitousek PM, Naylor R, Crews T, David MB, Drinkwater LE, Holland E, Johnes PJ, Katzenberger J, Martinelli LA, Matson PA *et al.* 2009. Agriculture. Nutrient imbalances in agricultural development. *Science* **324**: 1519–1520.

Voss-Fels KP, Stahl A, Wittkop B, Lichthardt C, Nagler S, Rose T, Chen T-W, Zetzsche H, Seddig S, Majid Baig M *et al.* 2019. Breeding improves wheat productivity under contrasting agrochemical input levels. *Nature Plants* **5**: 706–714.

Wang C, Qi Z, Zhao J, Gao Z, Zhao J, Chen F, Chu Q. 2023. Sustainable water and nitrogen optimization to adapt to different temperature variations and rainfall patterns for a trade-off between winter wheat yield and N_2O emissions. *Science of the Total Environment* **854**: 158822.

Wang H, Wan Y, Buchner P, King R, Ma H, Hawkesford MJ. 2020. Phylogeny and gene expression of the complete *NITRATE TRANSPORTER 1/PEPTIDE TRANSPORTER FAMILY* in *Triticum aestivum*. *Journal of Experimental Botany* **71**: 4531–4546.

Wang J, Lu K, Nie H, Zeng Q, Wu B, Qian J, Fang Z. 2018. Rice nitrate transporter OsNPF7.2 positively regulates tiller number and grain yield. *Rice* **11**: 12.

Wang R, Guan P, Chen M, Xing X, Zhang Y, Crawford NM. 2010. Multiple regulatory elements in the Arabidopsis *NIA1* promoter act synergistically to form a nitrate enhancer. *Plant Physiology* **154**: 423–432.

Wang S, Wong D, Forrest K, Allen A, Chao S, Huang BE, Maccaferri M, Salvi S, Milner SG, Cattivelli L *et al.* 2014. Characterization of polyploid wheat genomic diversity using a high-density 90,000 single nucleotide polymorphism array. *Plant Biotechnology Journal* **12**: 787–796.

Wilkinson JQ, Crawford NM. 1993. Identification and characterization of a chlorate-resistant mutant of *Arabidopsis thaliana* with mutations in both nitrate reductase structural genes NIA1 and NIA2. *Molecular and General Genetics MGG* **239**: 289–297.

von Wirén N, Gazzarrini S, Gojon A, Frommer WB. 2000. The molecular physiology of ammonium uptake and retrieval. *Current Opinion in Plant Biology* **3**: 254–261.

von Wittgenstein NJ, Le CH, Hawkins BJ, Ehlting J. 2014. Evolutionary classification of ammonium, nitrate, and peptide transporters in land plants. *BMC Evolutionary Biology* **14**: 11.

Xin W, Zhang L, Gao J, Zhang W, Yi J, Zhen X, Bi C, He D, Liu S, Zhao X. 2021. Adaptation mechanism of roots to low and high nitrogen revealed by proteomic analysis. *Rice* **14**: 5.

Xu G, Fan X, Miller AJ. 2012. Plant nitrogen assimilation and use efficiency. *Annual Review of Plant Biology* **63**: 153–182.

Yang JT, Schneider HM, Brown KM, Lynch JP. 2019. Genotypic variation and nitrogen stress effects on root anatomy in maize are node specific. *Journal of Experimental Botany* **70**: 5311–5325.

Yu J, Xuan W, Tian Y, Fan L, Sun J, Tang W, Chen G, Wang B, Liu Y, Wu W *et al.* 2021. Enhanced OsNLP4–OsNiR cascade confers nitrogen use efficiency by promoting tiller number in rice. *Plant Biotechnology Journal* **19**: 167–176.

Zhang Y, Ngu DW, Carvalho D, Liang Z, Qiu Y, Roston RL, Schnable JC. 2017. Differentially regulated orthologs in sorghum and the subgenomes of maize. *Plant Cell* **29**: 1938–1951.

Zhao M-G, Chen L, Zhang L-L, Zhang W-H. 2009. Nitric reductase-dependent nitric oxide production is involved in cold acclimation and freezing tolerance in Arabidopsis. *Plant Physiology* **151**: 755–767.

Zheng Z, Hey S, Jubery T, Liu H, Yang Y, Coffey L, Miao C, Sigmon B, Schnable JC, Hochholdinger F *et al.* 2020. Shared genetic control of root system architecture between *Zea mays* and *Sorghum bicolor*. *Plant Physiology* **182**: 977–991.

Supporting Information

Additional Supporting Information may be found online in the Supporting Information section at the end of the article.

Fig. S1 Root phenotyping apparatus, Epson root scanner with the WinRhizo software.

Fig. S2 Phylogenetic and sequence alignment of the NPF2.12 proteins.

Fig. S3 Relative expression of *TaNPF2.12 and HVNPF2.12* in shoots between the alleles exposed to high and low NO_3^- availability.

Fig. S4 NO_3^-–N determination in root and shoot in wheat and barley haplotype (Hap) groups.

Fig. S5 Expression and overexpression observed in the sample comparison.

Fig. S6 RNA sequencing analyses of the *TaNPF2.12* wild-type and mutant allele after 14-d exposed to high and low NO_3^-.

Methods S1 Supporting information for the Materials and Methods section.

Table S1 List and description of winter wheat association panel comprising 221 diverse germplasms across world-wide collection.

Table S2 List and description of spring barley association panel comprising 200 diverse germplasms across world-wide collection.

Table S3 N_{min} amounts (based on ha) of soil samples at 0–30, 30–60, and 60–90 cm soil depth (average values).

Table S4 Description of root system morphological and anatomical traits with trait acronyms and unit.

Table S5 List of nitrate transporter protein sequences identified in different crop species obtained from NCBI database.

Table S6 Promoter sequence variation of *TaNPF2.12* from 40 different wheat cultivars.

Table S7 Promoter sequence variation of *HvNPF2.12* from 40 different barley genotypes.

Table S8 Primers used for the DNA sequencing and expression analysis of *TaNPF2.12* in wheat cultivars.

Table S9 Primers used for the DNA sequencing and expression analysis of *HvNPF2.12* in barley genotypes.

Table S10 Descriptive statistics for investigated root morphology and anatomy traits in wheat association panel.

Table S11 Analysis of variance and broad-sense heritability (H^2) for investigated traits in wheat association panel.

Table S12 Descriptive statistics, analysis of variance and broad-sense heritability (H^2) for investigated traits in barley association panel.

Table S13 List of identified significant marker-traits associations in wheat genome under different N input levels in wheat panel.

Table S14 List of candidate genes associated with root system architectural traits at different N responses.

Table S15 List of nitrogen-associated genes in wheat and barley obtained by comparative genome-wide association studies.

Table S16 List of identified significant marker-traits association and underlying candidate genes in barley under different NO_3^- input levels.

Table S17 List of syntenic gene pairs that lies on chromosome 3 and highly associated with root system traits in both wheat and barley under LN/HN conditions.

Table S18 Summary of RNA-seq analysis and list of high confidential (HC) genes and their up and down-regulation patterns.

Table S19 List of significantly enriched pathways of differentially expressed genes (DEGs) in wild-type and npf2.12 mutant alleles under high and low nitrate treatments.

Please note: Wiley is not responsible for the content or functionality of any Supporting Information supplied by the authors. Any queries (other than missing material) should be directed to the *New Phytologist* Central Office.